Emergence of shape and flow structure in Nature in the light of Constructal Theory

A. Heitor Reis

Physics Department and Évora Geophysics Centre, University of Évora,

R, Romão Ramalho, 59, 7000-671, Évora, Portugal

Tel + 351 967324948;   Fax: +351 266745394;   e-mail: ahr@uevora.pt

1.1. Introduction

Constructal theory and the constructal law are terms that we see more and more in the current scientific literature. The reason is that increasing numbers of people use the constructal paradigm to optimize the performance of thermofluid flow systems by generating geometry and flow structure, and to explain natural self-organization and self-optimization. Constructal theory is a principle-based method of constructing machines, which attain optimally their objective. Constructal theory offers a different look at corals, birds, atmospheric flow and, of course, at machines in general.

There is an old history of trying to explain the forms of nature—why does a leaf have nerves, why does a flower have petals—this history is as old as people have existed. Geometry has focused on explaining form, and has contributed to much of the knowledge inherited from antiquity.

For the first time, engineers have entered an arena where until now the discussion was between mathematicians, physicists, biologists, zoologists. The engineers enter with a point of view that is very original, and which may enlighten the questions with which others have struggled until now.

Adrian Bejan is at the origin of the constructal paradigm, which had its start in 1996. In his books [1,2] he tells that the idea came to him when he was trying to solve the problem of minimizing the thermal resistance between an entire heat generating volume and one point. As the optimal solution, he found "a tree network in which every single feature was a *result*, not an assumption", and drew the conclusion that every natural tree structure is also the result of optimisation of performance of volume-point flow. As natural tree structures are everywhere, and such structures are not deducible from a known law, he speculated that the optimisation of configuration in time must be a *new* principle and called it the *constructal law*. He stated this law as follows: *For a finite-size system to persist in time (to live), it must evolve in such a way that it provides easier access to the imposed (global) currents that flow through it.*

A new statement deserves recognition as a principle only if it provides a conceptual framework for predicting form and evolution of form and for modelling natural or engineered systems. Bejan has not only formulated the constructal principle but also developed a method for applying it to practical situations. The *constructal method* (Bejan [1-6]) Bejan and Tondeur [7]) is about the generation of flow architecture in general (e. g. , duct cross-sections, spacings, tree networks). For example, the generation of tree-shaped architecture proceeds from small parts to larger assemblies. *The optimal structure is constructed by optimizing volume shape at every length scale, in a hierarchical sequence that begins with the smallest building block and proceeds towards larger building blocks (which are called "constructs").*

A basic outcome of constructal theory is that system shape and internal flow architecture do not develop by chance, but result from the permanent struggle for better performance and therefore must evolve in time. Natural systems that display an enormous variety of shapes are far from being perfect from the geometric point of view. Geometric perfection means symmetry (e. g., the sphere has the highest possible geometric symmetry) but in the physical (real) world the higher the internal symmetry the closer to equilibrium, to no flow, and death. We know that translational symmetry (invariance) with respect to temperature, pressure and chemical potential means thermal, mechanical and chemical equilibrium respectively, while translational angular invariance of the lagrangian means conservation of linear and angular momentum respectively (Noether's theorem).

Nevertheless, it is almost impossible to find the perfect geometric form in animate systems because they are far from equilibrium: they are alive, and imperfection (physical and geometrical asymmetry) is the sign that they are alive. Yet, they work "best" because they minimize and balance together the resistances faced by the various internal and external streams under the existing global constraints.

Non-equilibrium means flow asymmetry and imperfection. Imperfection is either geometric (e. g., quasi-cylindrical channels, quasi-spherical alveolus, quasi-circular stoma, etc.) or physical (unequal distribution of stresses, temperature, pressure, etc.). Therefore, internal imperfections are optimally distributed throughout the system (Bejan [1,2]). The actual form of natural systems that were free to morph in the past is the result of *optimal distribution of imperfection,* while engineered systems approach the same goal and structure as they tend to optimal performance.

The constructal law is self-standing and distinct from the second law (Bejan [1, 8, 9]). Unlike the second law that accounts for the one-way nature of flows (i.e., irreversibility), the constructal law is about the generation of *flow* configuration, structure, geometry. Its field of application is that of dissipative processes (flows that overcome resistances), entropy generation, and non-equilibrium thermodynamics. In recent papers, Bejan and Lorente [8, 9] outlined the analogy between the formalism of equilibrium thermodynamics and that of constructal theory (see section 6). In what follows, we outline the main features of constructal theory, and present an overview of recent developments and applications to various fields.

1.2. Constructal method

Constructal theory holds that every flow system exists with *purpose (or objective, function)*. In nature, flows occur over a wide range of scales with the purpose of reducing the existing gradients (temperature, pressure, etc.). In engineered and living structures heat and mass flows occur for the same reason, and by dissipating minimum exergy they reduce the food or fuel requirement, and make all such systems (animals, and "man + machine" species) more "fit", i.e., better survivors. They "flow" better and better, internally and over the surface of the earth.

The purpose of heat engines is to extract maximum useful work from heat currents that flow between systems at different temperatures. Other machines work similarly, i.e. with purpose, e.g. by collecting or distributing streams, or for enhancing heat or mass transfer. Performance is a measure of the degree to which each system realizes its purpose. The design of engineered systems evolves in time toward configurations that offer better performance, i.e. better achievement of their purpose.

The system purpose is global. It is present along with fixed global constraints, which may include the space allocated to the system, available material and components, allowable temperature, pressure or stress ranges, etc. The system designer brings together all components, and optimizes the arrangement in order to reach maximum performance. In this way he "constructs" the optimal flow architecture. Therefore, the flow architecture (shape, structure) is *deduced*, not assumed in advance. Unlike optimising procedures that rely on operational variables, constructal theory focuses on the construction of optimal flow architecture, internal and external.

Optimization makes sense only when purpose exists and the problem-solver has the *freedom* to morph the configuration in the search of the best solution within the framework of a set of constraints. The constraints may vary from allowable materials, material properties, area or volume allocated to the system, requirements to avoid hot-spots, or not to surpass maximal values of temperature, pressure, stresses, etc. Depending on the system's nature, optimization may focus on exergy analysis (e.g. Bejan [10, 11]), entropy generation (e.g. Bejan [12, 13]), thermoeconomics (e.g. Bejan et al. [14]) or minimization of highest stress, temperature or pressure (e.g. Bejan [2, 6], Bejan and Tondeur [7]).

The minimization of pressure peaks (Bejan [1, 2, 6], Bejan and Errera [15]) is a good way to illustrate the constructal method. The problem may be formulated as follows:

"A fluid has to be drained from a finite-size volume or area at a definite flow-rate trough a small patch located on its boundary. The flow is volume-point or area-point. It is a special and very important type of flow, because it connects one point with infinity of points. The volume is a non-homogeneous porous medium composed of a material of low permeability K and various layers of higher

permeabilities (K_o, K_1,..). The thicknesses (D_o, D_1,...) and lengths (L_o, L_1,....) of these layers are not specified. Darcy flow is assumed to exist throughout the volume considered. Determine the optimal arrangement of the layers through the given volume such that the highest pressure is minimized."

A first result is the use of the high permeability material where flow-rates are highest. Conversely, low permeability material shall be used for low flow rates. Next, we choose an elemental volume of length L_o and width H_o, filled with the low-permeability (K) isotropic porous medium (e.g. Fig. 1), and use higher permeability (K_o) material to drain the fluid from it. The area $A_o=H_oL_o$ of the horizontal surface is fixed but the shape H_o/L_o is not.

Because of symmetry and objective (optimization), the strip that collects fluid from the isotropic porous medium must be aligned with the x axis. And, because the flow-rate $\dot{m}'_0$ is fixed, to minimize the peak pressure means to minimize the global flow resistance. The peak pressure occurs in two corners (P, Fig. 1.1), and is given by:

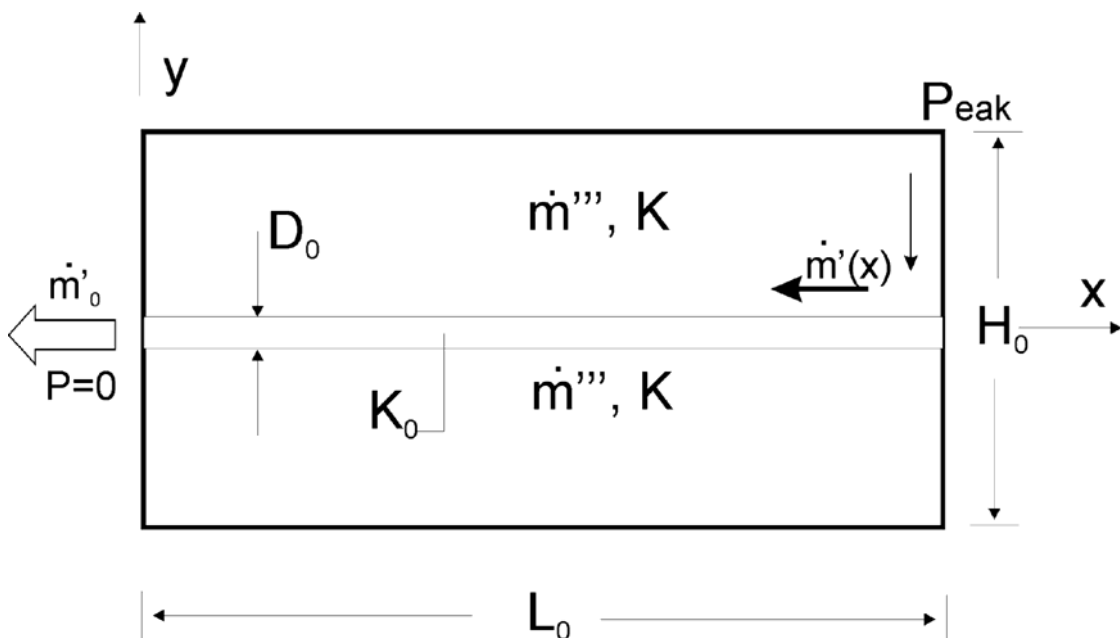$$P_{peak}=\dot{m}'_0\nu\left(H_0/8KL_0+L_0/2K_0D_0\right) \tag{1}$$

Fig. 1.1 - Elemental volume: the central high-permeability channel collects flow from low permeability material.

where D_0 represents the thickness of the central strip. By minimizing the peak pressure with respect to the shape parameter H_0/L_0 we find that the optimum geometry is described by:

$$\widetilde{H}_0 = 2^{1/2}\left(\widetilde{K}_0\phi_0\right)^{-1/4} \;\; ; \;\;\;\; \widetilde{L}_0 = 2^{-1/2}\left(\widetilde{K}_0\phi_0\right)^{1/4} \tag{2}$$

$$H_0/L_0 = 2\left(\widetilde{K}_0\phi_0\right)^{-1/2} \; ; \;\;\;\; \Delta\widetilde{P}_0 = 2^{-1}\left(\widetilde{K}_0\phi_0\right)^{-1/2} \tag{3}$$

where $\phi_0 = D_0/H_0 \ll 1$, $\Delta\widetilde{P}_0 = P_{peak}/(\dot{m}_0' A_0 \nu/K)$ and the symbol $\sim$ indicates nondimensionalized variables based on $(A_0)^{1/2}$ and K as length and permeability scales.

Equations (2) pinpoint the optimal geometry that matches minimum peak pressure and minimum resistance. The first of Eqs. (3) indicates another important result: the two terms on the right hand side of Eq. (1) are equal; said another way, "the shape of the elemental volume is such that the pressure drop along the central strip is equal to the pressure drop along the isotropic porous medium (K layer)". This is the constructal law of *equipartition of the resistances* (Bejan [1, 2], Bejan and Tondeur [7]). An analogous result for electric circuits was obtained by Lewins [16] who, based on the constructal theory, found an equipotential division between the competing regimes of low and high resistance currents.

Next, consider a larger volume (a "first construct") filled entirely with elemental volumes. This "first construct" is shown in Fig. 1.2.
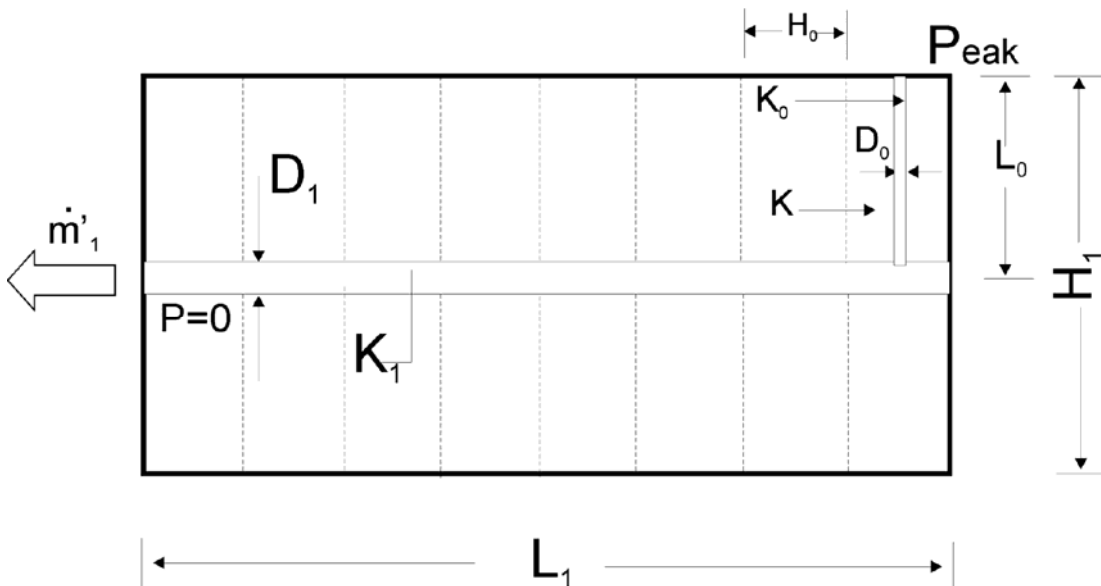

Fig. 1.2 - First construct made of elemental volumes. A new channel of higher permeability collects flow from the elemental volumes.

Once again, symmetry and objective dictate that the higher permeability strip that collects all the currents from the elemental volumes must be aligned with the horizontal axis of the first construct. The geometry of the first construct, namely the number n_1 of elemental volumes in the construct, is optimized by repeating the procedure used in the optimization of the elemental volume. If $C_i = \widetilde{K}_i \phi_i$, the parameters defining the optimized first construct are (Bejan [1]):

$$\widetilde{H}_1 = 2^{1/2}(C_0)^{1/4} \; ; \qquad \widetilde{L}_1 = C_0^{-1/4} C_1^{1/2} \tag{4}$$

$$H_1/L_1 = (2C_0/C_1)^{1/2} ; \qquad \Delta\widetilde{P}_1 = (2C_0/C_1)^{-1/2} \tag{5}$$

$$n_1 = (2C_1)^{1/2} \tag{6}$$

Higher order constructs can be optimized in a similar way until the specified area is covered completely. What emerges is a two-dimensional fluid tree in which optimization has been performed at every volume scale. The fluid tree is the optimal solution to two problems: the flow architecture that matched the lowest peak pressure, and the one that matched to lowest pressure averaged over the tree.

The constructal law can also be used in the same problem by basing the optimization on minimizing the pressure averaged at each scale of the fluid tree. Three-dimensional fluid trees may be in an optimized analogous manner (Bejan [1, 2, 6]). The same procedure applies to heat transfer trees (Bejan [1-3], Bejan and Tondeur [7], Bejan and Dan [17, 18], Ledezma and Bejan [19]).

1.3. Optimisation as a trade-off between competing trends

There are two competing trends in the example of section 2. Increasing in the length L_o of the central strip leads to a decrease in the resistance posed to flow in the K layer, but it also increases the resistance along the central channel (cf. Eq. (1)). Optimization meant finding the best allocation of resistances, and therefore the geometry of the system that allows best flow access from the area to the outlet. The law of equipartition of pressure losses summarizes the result of optimization of such flow access.

The optimum balance between competing trends is at origin of "equilibrium" flow architectures in both engineered and natural systems, and is in the domain of constructal theory. Like the thermodynamic equilibrium states that result from the maximization of entropy (or the minimization of free energy) in nonflow systems

in classical thermodynamics, equilibrium flow architectures spring out of the maximization of flow access (Bejan and Lorente [8,9]).

Consider the following example of optimization under competing trends. Air at temperature T_o is made to flow at rate $\dot{m}$ through a set of equidistant heat generating boards of length L and width W (perpendicular to the plane of the figure) filling a space of height H (Fig. 1.3).

The board-to-board spacing D, is to be determined in order to maximize the rate q at which heat is removed. As a local constraint, the temperature must not exceed a specified value, T_{max}. Other assumptions are laminar flow, smooth board surfaces, and that the temperature along every board is close to T_{max}.

Small board-to-board spacings permit a large number of boards $(n=H/D)$ to be installed and cooled. Although in this limit the contact heat transfer area is large, the resistance to fluid flow is also large. The optimal spacing D_{opt} must come out of the balance between these two competing trends, fluid flow resistance against thermal resistance.
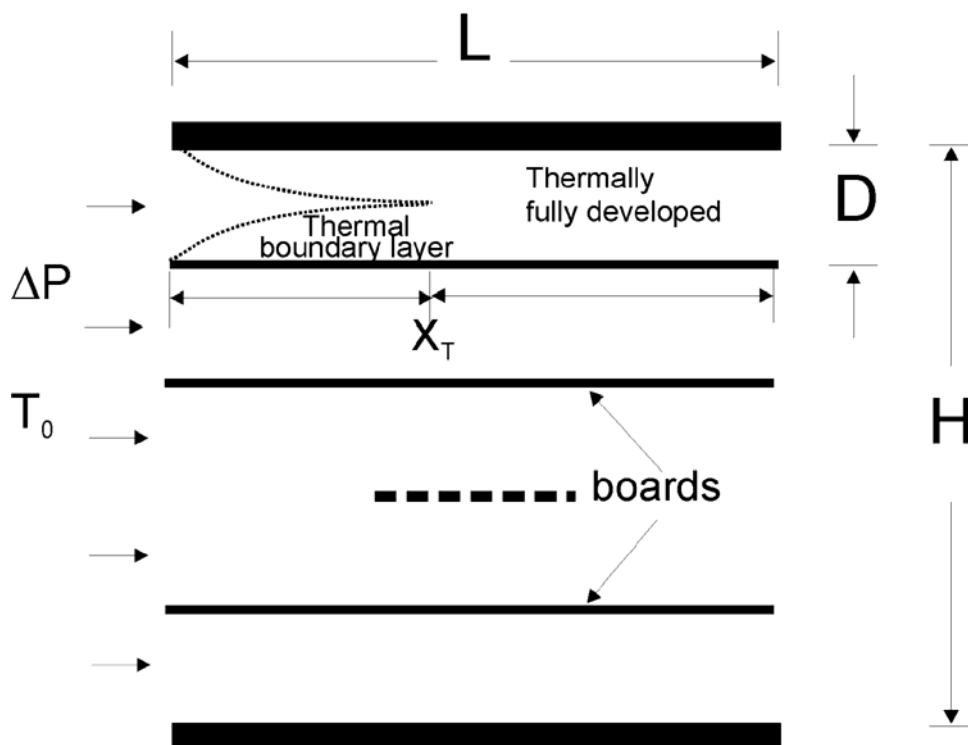

Fig. 1.3 -   The optimal spacing comes out of the trade-off between heat transfer surface and resistance to fluid flow. Board to board spacing is optimal when every fluid volume is used for the purpose of heat transfer.

For very small spacings (large n) the heat transfer rate is (Bejan [1]):

$$q = \rho HW \left(D^2/12\mu\right)\left(\Delta P/L\right) c_p \left(T_{max} - T_0\right) \tag{7}$$

where ρ, μ and c_p stand for density, viscosity and specific heat, respectively. For large spacing (small *n*), each plate is coated by distinct boundary layers, and the heat transfer rate is given by [1]:

$$q = 1.21kHW \left[Pr \, L\Delta P/\left(\rho \nu^2 D^2\right)\right]^{1/3} \left(T_{max} - T_0\right) \tag{8}$$

where *k*, ν and *Pr* are thermal conductivity, kinematic viscosity and Prandlt number, respectively.

Equation (7) shows that the heat transfer rate *q* increases asymptotically with D^2 as *n* becomes smaller (Eq. 7), while when *n* becomes larger it varies asymptotically as $D^{-2/3}$ (Eq. 8). Therefore, the number of boards for which the heat transfer rate is maximum can be determined approximately by using the method of intersecting the asymptotes (Bejan [1, 20, 21], as shown in Fig. 1.4.
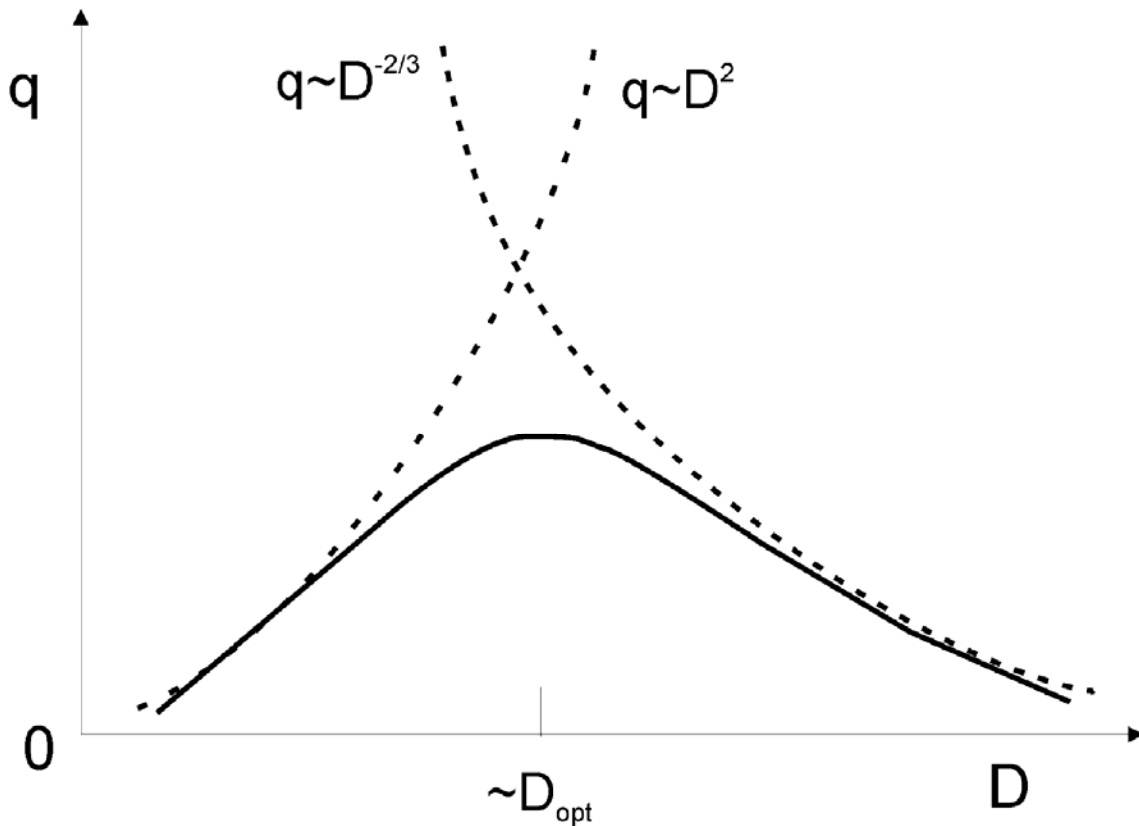

Fig. 1.4 – The intersection of the asymptotes corresponding to the competing trends indicates the optimum spacing for maximum thermal conductance of a stack of parallel boards.

The optimal spacing is given by:

$$D_{opt}\big/L \propto Be^{-1/4} \qquad\qquad\qquad\qquad (9)$$

where $Be=(\Delta PL^2)/(\mu\alpha)$ is what Bhattacharjee and Grosshandler [22] Petrescu [23] called the Bejan number.

The spacing defined by Eq. (9) is not only the optimal solution to maximum heat transfer while keeping the temperature below T_{max}, but also is the solution to the problem of packing maximum heat transfer rate in a fixed volume. The best elementary construct to this second problem is a heat transfer board whose length matches the entrance length X_T (see Fig. 3). Maximum packing occurs when every packet of fluid is used for transferring heat. If $L < X_T$, the fluid in the core of the channel does not interacts thermally with the walls, and therefore does not participate in the global heat transfer enterprise. In the other extreme, $L > X_T$, the flow is fully developed, the fluid is saturated thermally and it overheats as it absorbs additional heat from the board walls.

The optimal spacing determined in this manner enables us to see the significance of the Bejan number. In steady conditions, the rate at which heat is transferred from the boards to the fluid, $\bar{h}(T_{max}-T_0)WL$, must equal the rate of enthalpy increase $\rho v c_p (T_{max}-T_o)DW$, where $v=[(\Delta P)D^2]/(12\mu)$, which is removed by the cooling fluid that flows under the pressure difference ΔP. Therefore, for $L_{opt} = X_T$ this equality of scales reads:

$$Be = 12\bar{N}u_D\big(L_{opt}\big/D_{opt}\big)^4 \qquad\qquad\qquad (10)$$

which matches Eq. (9). In Eq. (10), $\bar{N}u_D = \bar{h}D/k =(\partial T^*/\partial z^*)$ is Nusselt number based on D_{opt} (where $T^*=T/(T_{max}-T_o)$ and $z^*=z/D_{opt}$), which is a constant of order 1.

By analogy with section 2, optimized convective heat trees can be constructed at every scale by assembling and optimizing constructs that have been optimized at the preceding scale (Bejan [1], Ledezma and Bejan [19]). Similarity exists between the forced convection results and the corresponding results for natural convection. The role played by Bejan number Be in the forced convection is played in natural convection be the Rayleigh number Ra (Petrescu [23]).

1.4. The ubiquitous search for flow configuration: fields of application of Constructal Theory

Flow architectures are ubiquitous in Nature. From the planetary circulations to the smallest scales we can observe a panoply of motions that exhibit organized flow architectures: general atmospheric circulations, oceanic currents, eddies at the synoptic scale, river drainage basins, dendritic crystals, etc. Fluids circulate in all living structures, which exhibit special flow structures such as lungs, kidneys, arteries and veins in animals, and roots, stems, leaves in plants (Fig.5),

Transportation networks where goods and people flow have been developed on the purpose of maximum access - best performance in economics and for facilitating all human activities. Similarly, internal flow structures where energy, matter and information flow are at the heart of engineered systems.

Flow architectures in both living and engineered systems evolve toward better performance, and persist in time (they survive) while the older disappear (Bejan [1, 24, 25]. This observation bridges the gap between the constructal law and the darwinian view of living systems. Results of the application of constructal theory have been published in recent years for various natural and engineered systems (Reis [25]). In the following, we review briefly some examples of application of constructal theory.

References

[1] A. Bejan, *Shape and Structure, from Engineering to Nature*, Cambridge University Press, Cambridge, UK, 2000.

[2] A. Bejan, *Advanced Engineering Thermodynamics*, Second Edition, Wiley, New York, 1997, ch. 13.

[3] A. Bejan, "Constructal-Theory Network of Conducting Paths for Cooling a Heat Generating Volume," *International Journal of Heat and Mass Transfer*, Vol. 40, 1997, pp. 799-816.

[4] A. Bejan, "Theory of Organization in Nature: Pulsating Physiological Processes," *International Journal of Heat and Mass Transfer*, Vol. 40, 1997, pp. 2097-2104.

[5] A. Bejan, "How Nature Takes Shape," Mechanical Engineering, Vol. 119, No. 10, October 1997, pp. 90-92.

[6] A. Bejan, "Constructal Tree Network for Fluid Flow between a Finite-Size Volume and One Source or Sink," *Revue Générale de Thermique*, Vol. 36, 1997, pp. 592-604.

[7] A. Bejan and D. Tondeur, "Equipartition, Optimal Allocation, and the Constructal Approach to Predicting Organization in Nature" *Revue Générale de Thermique*, Vol. 37, 1998, pp. 165-180.

[8] A. Bejan and S. Lorente "The constructal law and the themodynamics of flow systems with configuration", *International Journal of Heat and Mass Transfer*, Vol. 47, 2004, pp. 3203-3214.

[9] A. Bejan and S. Lorente, "Equilibrium and Nonequilibrium Flow System Architectures", *International Journal of Heat & Technology*, Vol. 22, No. 1, 2004, pp. 85-92.

[10] A. Bejan, "A Role for Exergy Analysis and Optimization in Aircraft Energy-System Design," *ASME AES*-Vol. 39, 1999, pp. 209-218.

[11] A. Bejan, "Fundamentals of Exergy Analysis, Entropy Generation Minimization, and the Generation of Flow Architecture", *International Journal of Energy Research*, Vol. 26, No. 7, 2002, pp. 545-565.

[12] A. Bejan, *Entropy Generation Through Heat and Fluid Flow*, Wiley, New York, 1982.

[13] A. Bejan, *Entropy Generation Minimization*, CRC Press, Boca Raton, 1996.

[14] A. Bejan, V. Badescu and A. De Vos, "Constructal Theory of Economics Structure Generation in Space and Time" *Energy Conversion and Management*, Vol. 41, 2000, pp. 1429-1451.

[15] A. Bejan and M. R. Errera, "Deterministic Tree Networks for Fluid Flow: Geometry for Minimal Flow Resistance between a Volume and One Point," *Fractals*, Vol. 5, No. 4, 1997, pp. 685-695.

[16] J. Lewins, "Bejan's constructal theory of equal potential distribution", *International Journal of Heat and Mass Transfer*, 46, 2003, pp. 1451-1453.

[17] A. Bejan and N. Dan, "Two Constructal Routes to Minimal Heat Flow Resistance via Greater Internal Complexity," *Journal of Heat Transfer*, Vol. 121, 1999, pp. 6-14.

[18] A. Bejan and N. Dan, Constructal trees of convective fins", *Journal of Heat Transfer*, 121, 1999, pp. 675-682.

[19] G. A. Ledezma and A. Bejan, "Constructal Three-Dimensional Trees for Conduction between a Volume and One Point," *Journal of Heat Transfer*, Vol. 120, November 1998, pp. 977-984.

[20] A. Bejan, *"Convection Heat Transfer"* 3rd Ed. 2004, Wiley, New York.

[21] A. Bejan, "Simple Methods for Convection in Porous Media: Scale Analysis and the Intersection of Asymptotes", *International Journal of Energy Research*, Vol. 27, 2003, pp. 859-874.

[22] S. Battacharjee and W. L. Grosshandler, "The formation of a wall jet near a high temperature wall under microgravity environment, *ASME HTD*, 96, 1988, pp. 711-716.

[23] S. Petrescu, "Comments on the optimal spacing of parallel plates cooled by forced convection", *International Journal of Heat and Mass Transfer*, 37, 1994, p. 1283.

[24] A. Bejan, "How Nature Takes Shape: Extensions of Constructal Theory to Ducts, Rivers, Turbulence, Cracks, Dendritic Crystals and Spatial Economics," *International Journal of Thermal Sciences* (Revue Générale de Thermique), Vol. 38, 1999, pp. 653-663.

[25] A. Bejan, "Constructal Theory: An Engineering View on the Generation of Geometric Form in Living (Flow) Systems", *Comments on Theoretical Biology*, Vol. 6, No. 4, 2001, pp. 279-302.

[26] A. Heitor Reis, 2006, "Constructal Theory: From Engineering to Physics, and How Flow Systems Develop Shape and Structure", *Applied Mechanics Reviews*, Vol.59, Issue 5, pp. 269-282.

2. Architectures of particle agglomeration

2.1. Introduction

The objective of this paper [1] is to bring to the attention of aerosol researchers a new physics principle – the constructal law [2, 3] – the implications of which are general and important in natural, industrial and biological systems [3, 4]. Constructal theory is about the phenomenon of generation of architecture in flow systems. The acquisition of geometry is the mechanism by which the system meets its global objectives under the existing constraints. The objective is the maximization of global access for all the currents that flow through the system. Flow resistances cannot be eliminated. They can be balanced against each other, so that their global effect is minimized. This evolutionary process of balancing and distributing resistances constitutes the generation of flow configuration. The resulting (constructal) configuration is deduced from principle, not assumed, and not postulated.

The global maximization of flow access predicts in simple manner not only the evolution of man-made systems but also the shapes and structures that occur in nature. The rapid development of constructal theory was reviewed by several authors [3 – 7].

In this paper we use constructal theory to describe the morphology of agglomerates of particles.

2.2. Shape and structure of agglomerates of particles

Agglomeration is the process by which particles collide to form larger particles, which typically have greater settling speed. Deposition describes the process by which particles collide and attach to surfaces. Collisions and the coming together of multiple particles result in aggregates that usually have dendritic shape. This pattern of agglomeration and deposition has a profound effect on filtration process, nano-materials processing and the performance of such devices [8, 9].

Agglomerates of aerosol particles often have dendritic shapes that can be observed experimentally [9] or based on numerical simulations [10 – 13]. Is dendritic shape the prevalent and natural form of particle agglomeration? If so, why do aggregates of particles exhibit this particular shape?

Here we address these issues in the framework provided by constructal theory

[2]. The *constructal law requires the architecture of the aggregate of particles to evolve in time in such a way that the global rate of accumulation of the particles is maximized.* The generation of optimized architectures should bring the entire flow system (ambient + particles) to equilibrium in the fastest way.

Consider the following illustration of why the occurrence of dendritic agglomerates can be anticipated by the constructal law. The forces that make aerosol particles stick onto collectors (filter/beds/previously deposited particles) are of the electrical type. In fact, it is impossible to find electrically neutral surfaces in contact with air. Electrical bonds may occur through interactions of various types (e.g. charge-charge, charge-dipole, dipole-dipole, etc.). However, charge-charge interactions cancel the existing surface charge, and only the charge-dipole interaction ensures a steady and continuing process of deposition, because a dipole-charge bond leaves the total charge amount invariant (Fig. 2.1).

This is a very common form of interaction because almost all particles have significant dipolar moments.

Assume that a spherical surface with a surface charge density σ collects particles from a surrounding cloud of dipolar particles having uniform concentration C_p in stagnant air.
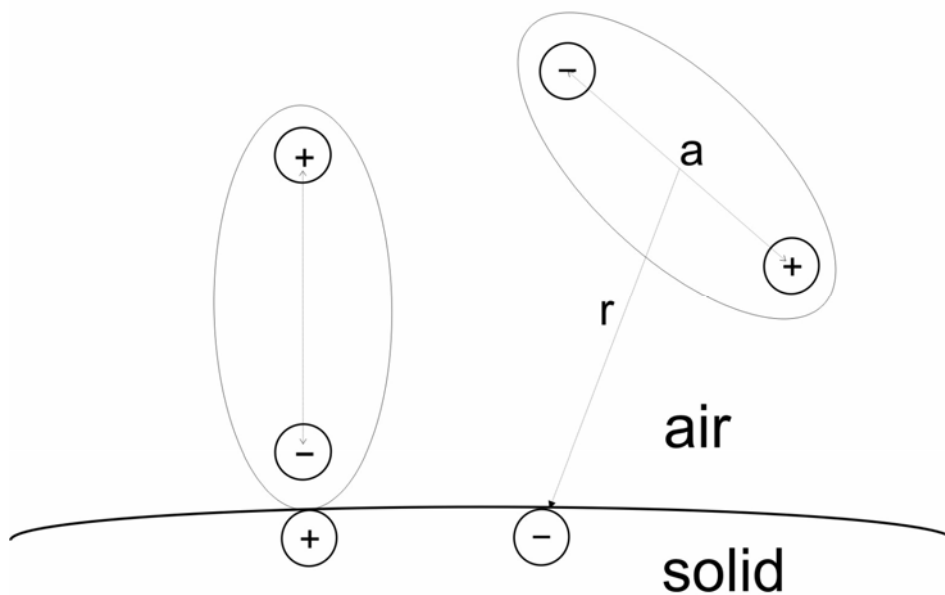

Fig 2.1. Dipolar particles near a charged surface.

Before binding to the surface, the small particles travel radially under the influence of charge-dipole forces. For a very small particle travelling with a Stokes flow velocity u_p, the drag force F_D is

$$F_D = \frac{3\pi\eta d_p u_p}{c_c}$$

(1)

Here η is the dynamic fluid viscosity, d_p is the particle diameter and c_c is the Cunningham correction factor [8]. The charge-dipole force F_C of attraction between the surface and a particle of dipolar moment $\vec{\mu} = q\vec{a}$ is

$$F_C = \frac{1}{4\pi\varepsilon_0} \frac{\int_A \mu\sigma \cos\alpha \, dA}{r^3}$$

(2)

where ε is the electric permittivity of the air, and r is the distance between the dipole centre and the surface charge (Fig. 2.2). The evaluation of F_C may be carried out for the cases of spherical, cylindrical, and planar geometries in the following way:

For spherical geometry, by considering Fig. 2, one has the following relationships:

$$r \sin\theta = R \sin\varphi$$

(3)

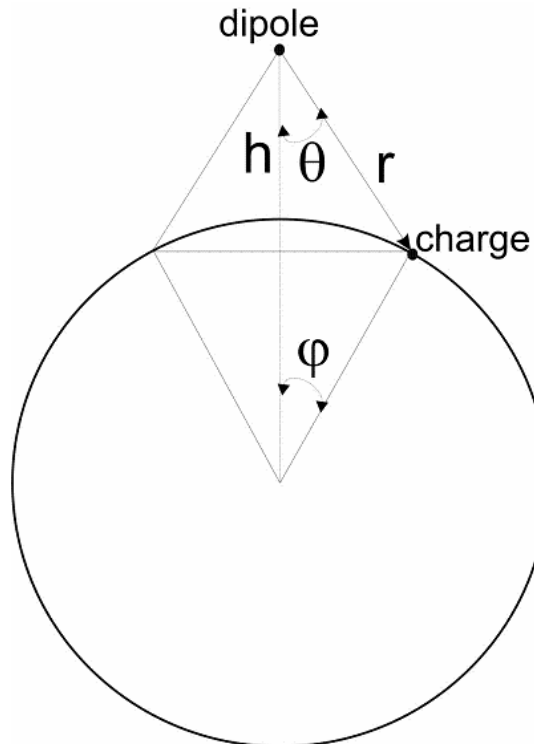$$r \cos\theta + R \cos\varphi = R + h$$

(4)

Fig. 2.2 Interaction between dipole and a charged (spherical or cylindrical) surface.

In order to evaluate the charge-dipole force in the vicinity of the surface we consider $h \sim a/2$, $\sin \theta \sim 1$. Half of dipolar particles are repelled from the surface while the other half is attracted to the surface. The mean value of $\cos \alpha$ is $2 / \pi$. Therefore the mean attractive force between surface charges and dipole (see Eq. 2) reads:

$$F_{Csp} \sim \frac{\mu \sigma}{\pi \varepsilon_0 R} \int_0^{\varphi_0} \frac{d\varphi}{\sin^2 \varphi} \tag{5}$$

After evaluating the integral in (5) and with $\sin \varphi_0 \sim (h / R)^{1/2}$, $h \sim a/2$, $\mu = qa$, and $R = D/2$, one has:

$$F_{Csp} \sim \frac{\sigma}{\pi \varepsilon_0} (q\mu)^{1/2} D^{-1/2} \tag{6}$$

For the cylindrical geometry with $\cos \varphi_0 \sim 1$, Eq. (2) reads:

$$F_{Ccy} \sim \frac{\mu \sigma}{2\pi^2 \varepsilon_0 R} \int_0^{\varphi_0} d\varphi \int_{-\infty}^{+\infty} \frac{d(L/R)}{\left(L^2/R^2 + \sin^2 \varphi\right)^{3/2}} \tag{7}$$

or, with $d = R/2$

$$F_{Ccy} \sim \frac{2\sigma}{\pi^2 \varepsilon_0} (q\mu)^{1/2} d^{-1/2} \tag{8}$$

Finally, for the force between dipole and planar charged surface one has:

$$F_{Cpl} = \frac{2\sigma\mu}{\pi \varepsilon_0} \int_0^{\pi/2} \frac{\sin \theta \cos^2 \theta d\theta}{a} \tag{9}$$

or

$$F_{Cpl} = \frac{2\sigma q}{3\pi \varepsilon_0} \tag{10}$$

We assume that both forces, F_D and F_C, cancel each other so that just before particles bind to the surface they travel with the velocity u_p. Hence, from Eqs. (1) and (6) we may calculate the flux of particles ($\dot{n}_{sp} = C_p u_p / 2$, where C_p is the concentration of dipolar particles in the vicinity of the surface) toward the surface of the sphere as

$$\dot{n}_{sp} = \frac{K}{v_p} D^{-1/2} \tag{11}$$

where

$$K = \frac{C_p \sigma c_c v_p}{6\pi^2 \varepsilon_0 \eta d_p} (q\mu)^{1/2} \tag{11a}$$

By using Eqs. (1) and (8), for a cylindrical surface of diameter d we calculate the flux of particles ($\dot{n}_{cy} = C_p u_p / 2$) toward the surface as:

$$\dot{n}_{cy} = \frac{2K}{\pi v_p} d^{-1/2} \tag{12}$$

while, with the help of Eqs. (1) and (10) the flow of particles toward a planar charged surface reads

$$\dot{n}_{pl} = \frac{2K}{3v_p} \left(\frac{q}{\mu}\right)^{1/2} \tag{13}$$

Both spherical and cylindrical modes of agglomeration can occur in nature. The competition between these two modes is the origin of the dendritic shape that occurs throughout nature.

The constructal law requires the architecture of the agglomerate to evolve in time in such a way that the global rate of accumulation of the particles is maximized. The total current of particles ($\dot{N}_{sp} = A_{sp} \dot{n}_{sp}$), that bind to a spherical surface (area $A_{sp} = \pi D^2$) is

$$\dot{N}_{sp} = \frac{\pi K}{2v_p} D^{3/2} \tag{14}$$

while the total current of particles that bind to a cylindrical surface (length L, area $A_{cy} = \pi d L$) is given by:

$$\dot{N}_{cy} = \frac{2K}{v_p} L d^{1/2} \tag{15}$$

While from Eq. (13) we see that the flux toward a planar surface depends only on surface charge density and dipole moment, Eqs. (14) and (15) show that the particle binding rate also depends on the geometry of the agglomerate. For the case of a spherical agglomerate we note that $\dot{N}_{sp} = \left(\pi / 2 v_p\right) D^2 \dot{D}$, and after using Eq. (14) we obtain:

$$D = \left(\frac{3K}{2}\right)^{2/3} t^{2/3} \tag{16}$$

On the other hand, for a cylinder of fixed length L with $\dot{N}_{cy} = \left(\pi/2v_p\right) Ld\dot{d}$, we obtain from Eq. (15):

$$d = \left(\frac{6K}{\pi}\right)^{2/3} t^{2/3} \tag{17}$$

Next, we use Eq. (16) to calculate the volume of the spherical agglomerate,

$$V_{sp} = \frac{3\pi K^2}{8} t^2 \tag{18}$$

Cylindrical growth may develop from a disc, as shown in Fig. 3.

As the diameter increases with time (see Eq. 17) the agglomerate becomes conically shaped (Fig. 2.3). In this case the growth speed along the axis is given by $\dot{L} = \dot{n}_{pl} v_p$. Then, by using Eq. (13) we obtain

$$\dot{L} = \frac{2K}{3} \left(\frac{q}{\mu}\right)^{1/2} \tag{19}$$

Using Eqs. (17) and (19) and integrating with respect to time, we find the volume of the conically shaped agglomerate

$$V_{co} = \frac{3}{7} \left(\frac{6}{\pi}\right)^{1/3} \left(\frac{q}{\mu}\right)^{1/2} (Kt)^{7/3} \tag{20}$$
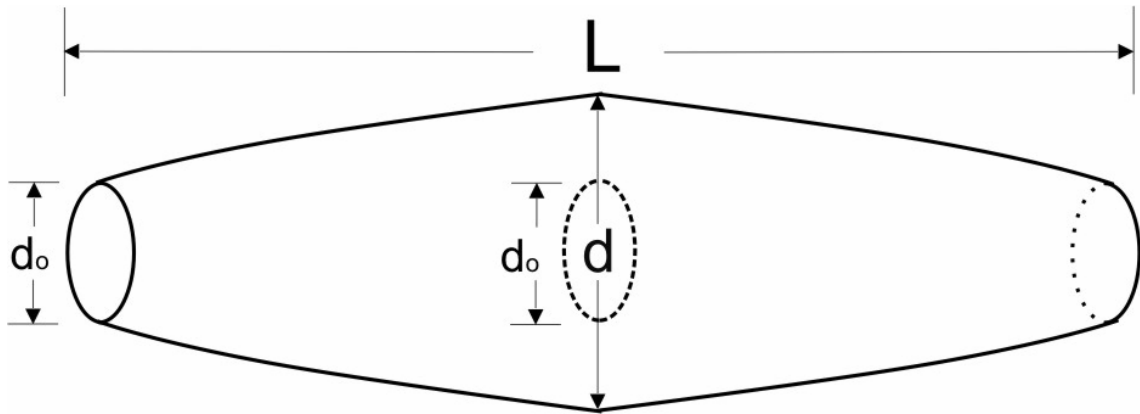

Fig. 2.3 Needle shaped agglomeration of particles.

From Eqs. (18) and (20) we see that the ratio

$$\frac{V_{sp}}{V_{co}} = \frac{2.2}{K^{1/3}} \left(\frac{\mu}{q}\right)^{1/2} t^{-1/3} \qquad (21)$$

is initially very high, and that it approaches o as t becomes sufficiently large. According to the constructal law this means that the agglomerate first must grow as a sphere, and change to the conical shape at a critical time later in its development. From Eq. (21) we see that for

$$t > \frac{9.9}{K} \left(\frac{\mu}{q}\right)^{3/2} \qquad (22)$$

the conically shaped agglomerate is more efficient as a particle collector than the spherically shaped agglomerate.

For water nucleating in ambient air, K is of order $10^{-11} \mathrm{m}^{3/2} \mathrm{s}^{-1}$ (which corresponds to a surface/water vapor field of order 10^{-2} μV m^{-1}) and $(\mu/q)^{1/2} \sim 10^{-4} m$. Therefore, the critical time for switching between spherical and conical growth as a preferential mode of agglomeration is of order 1 s, which corresponds to $D \sim 10^{-7}$ m for the diameter of the agglomerate. It is also interesting to compare the growth speeds of cone diameter and cone tip. By using Eqs. (17) and (19) we obtain:

$$\frac{\dot{d}}{\dot{L}} = \left(\frac{36}{K}\right)^{1/3} \left(\frac{\mu}{q}\right)^{1/2} t^{-1/3} \qquad (23)$$

which decreases as $t^{-1/3}$. This means that at later stages the agglomerate grows as a needle, the geometry of which is obtained from Eqs. (17) and (19) (Fig. 3)

$$d = \left(\frac{9}{\pi}\right)^{2/3} \left(\frac{\mu}{q}\right)^{1/3} L^{2/3} \qquad (24)$$

As an example, dendritic snow crystals have a length scale of order 10^{-3} m, and, by taking into account Eq. (24), we find $d / L \sim 10^{-2} L^{-1/3}$, which for $L \sim$ 1 mm yields $d/L \sim 10^{-2}$. This agrees with the order of magnitude of the diameter/length ratio of snowflake needles. Moreover, following Eq. (19) the needle tip growth speed is constant in accordance with experimental results [18].

One interesting aspect of the geometry predicted in Eq. (24) is that it depends only on the dipole moment μ. This means that weakly dipolar molecules will

agglomerate in a needle that is more slender than the needle formed by strongly dipolar molecules.

Another noteworthy aspect is that the critical time for switching from spherical to needle shaped growth depends only on the dipole strength, cf. Eq. (24). From Eqs. (16) and (22) we calculate the critical diameter of the original sphere as

$$D_{crit} \sim 6\frac{\mu}{q} \sim 6a \qquad (25)$$

This means that a universal behaviour of particle agglomeration exists: when the sphere diameter reaches 6 particle diameters, the agglomerate (of $(\pi/6)\times6^3 \sim 113$ particles) must switch from spherical to needle-shaped growth as a preferential mode of particle agglomeration.

Secondary needles may grow from specific points of the needle surface, generating in this way dendritic-growth architectures. A heat diffusion mechanism for explaining dendritic growth in snowflakes was proposed in [3].

In summary, the constructal law enables us to predict important features of shape generation and architecture of particle agglomeration. In the very beginning the agglomerate grows as a sphere, because at short times this shape is more effective in collecting particles from the environment.

There are many natural flow systems for which the architecture was proven to be optimized in accordance with the constructal law. Examples include the respiratory tree [15], river basins [5, 6], bacterial growth [5], patterns of cracks on the ground [3], and dendritic crystal growth [3, 16].

2.3. Concluding remarks

We showed that structure of particle agglomeration is generated in the pursuit of the equilibrium in the fastest way (constructal law) i.e., trough the maximization of particle agglomeration rate. At small times, spherical agglomeration of particles around a particle collector is the most effective mechanism. After a critical time the configuration switches from spherical symmetry to needle-shaped agglomeration, which performs best as a particle collector at long times. Secondary needle developments give rise to dendritic patterns. It was shown that the shape of the needle depends on the dipolar moment of the particles and that the critical number of particles in the spherical agglomerate before switching to needle shape does not

depend on the particle properties.

Nomenclature

a – spacing between charges (dipole), m
A – area, m^2
B – pressure drop number
c_c – Cunningham factor
C – concentration, kg m^{-3}
d – diameter of cylinder or distance, m
$\dot{d}$ – speed of diameter growth, m s^{-1}
D – diameter of sphere, m
D_{df} – diffusion coefficient, m^{2}s^{-1}
D_h – hydraulic diameter, m
F – force, N
H – height, m
K – constant (Eq. 11), m$^{5/2}$ s^{-2}
L – length, m
$\dot{L}$ – speed of needle tip growth, m s^{-1}

m – particle transfer density, kg m^{-3} s^{-1}
$\dot{n}$ – flux of particles, s^{-1}m^{-2}
$\dot{N}$ – current of particles, s^{-1}
p – pressure, Pa
P_o – Poiseuille number
q – charge, C
Re – Reynolds number
Sc – Schmidt number
Sh – Sherwood number
t – time, s
U – velocity, ms^{-1}
V – volume, m^3
H, L, W – height, length, width, m
Z – wetted perimeter, m

Greek Symbols
α, φ, θ – angle, rad
ε – porosity
ε_o – electric permittivity, C^{2}N^{-1}m^{-2}
ϕ – number of tubes/plates
η – viscosity, N s m^{-2}
κ – permeability, m^2

λ – particle transfer coefficient, ms^{-1}
μ – dipole moment, C m
ρ – air density, kg m^{-3}
σ – surface density of charge, C m^{-2}
τ – shear stress, Nm^{-2}

Subscripts
C – charge/dipole
cy – cylinder
D – drag

op – optimized
p – particle
pl – plane

References

[1] A. H. Reis, A. F.Miguel, and A. Bejan, 2006, , *Journal of Physics D: Applied Physics*, **39**, 2311-2318
[2] A. Bejan, *Advanced Engineering Thermodynamics*, chapter 13, 2nd edn. (Wiley, New York, 1997).
[3]A. Bejan, *Shape and Structure, from Engineering to Nature* (Cambridge University Press, Cambridge, 2000).
[4] A. Bejan, I. Dincer, S. Lorente, A. F. Miguel and A. H. Reis, *Porous and Complex Flow Structures in Modern Technologies* (Springer, New York 2004).
[5] R. N. Rosa, A. H. Reis and A. F. Miguel, *Bejan's Constructal Theory of Shape and Structure* (Ed. University of Evora, Center of Geofisica of Evora, Portugal, 2004).
[6] A. H. Reis, 2006 *Geomorphology*, Vol. **78**, 201-206.
[7] A. H. Reis, 2006, , *Applied Mechanics Reviews*, Vol.59, Issue 5, pp. 269-282.
[8] O. Filippova and D. Hänel, Journal of Aerosol Science **27**, S627 (1996)
[9] M. J. Lehmann and G. Kasper, in *Proceedings of the International workshop on particle loading and kinetics of filtration in fibrous filters* (Institut für Mechanische Verfahrenstechnik und Mechanik, Universität Karlsruhe, Germany, 2002).
[10] G. Yang and P. Biswas, J. Colloid Interface Sc. **211**, 142 (1999).

[11] C. Kanaoka, in *Advances in Aerosol Filtration,* edited by K. R. Spurny (CRC Press LCC. Washington, 1998), p. 323.

[12] R. Przekop, A. Moskal and L. Gradon, Journal of Aerosol Science **34**, 133 (2003).

[13] O. Filippova and D. Hänel, Computers and Fluids **26**, 697 (1997).

[14] K. G. Libbrecht, Rep. Prog. Phys. **68,** 855 (2005).

[15] A. H. Reis, A. F. Miguel and M. Aydin, Medical Physics **31**, 1135 (2004).

[16] A. Bejan, Revue Générale de Thermique **38**, 653 (1999).

sp – sphere

3. Flow architecture of the lungs

3.1 Introduction

The Constructal Principle that has been originally formulated by Adrian Bejan states that every system with internal flows develops the flow architecture that maximizes the heat and mass flow access under the constraints posed to the flow. In all classes of flow systems (animate, inanimate, engineered) the generation of flow architecture emerges as a universal phenomenon. This has been shown in a number of articles by Bejan and is summarized in a recent book [1].

By using the Constructal Principle, Bejan has addressed the rhythm of respiration in animals in relation with the body size and found that the breathing time increases with the animal body size rose to a power of 1/4, which is in good agreement with the biological observations.[1] A number of other recent studies have focused either on the characteristics of the airflow and gas diffusion within the lungs [2-6] and the form of the arterial bifurcations [6, 7] or statistical description of the respiratory tree [8,9].

In this work [15] we focus on the structure of the pulmonary airflow tree. The respiratory system is basically a fluid tree that starts at the trachea and bifurcates 23 times before reaching the alveolar sacs [4, 10] The reason for the existence of just 23 bifurcations in the respiratory tree (Fig. 3.1) has remained unexplained in the literature. Has this special flow architecture been developed by chance or does it represent the optimum structure for the lung's purpose, which is the oxygenation of the blood? The view that the Constructal Law which has been originally developed for engineered systems, holds also for living systems will guide us in finding the best airflow architecture for the respiratory system.

3.2 A fluid tree with purpose

The oxygenation of blood takes place in the tissues that shape the surface of the alveolar sacs. High alveolar surface promotes better oxygenation, but requires increased access to the external air. In fact, if the access to the external air faces high flow resistance the rate of oxygen diffusion into the blood is lowered due to the poor oxygen concentration in the air within the alveolar sacs.
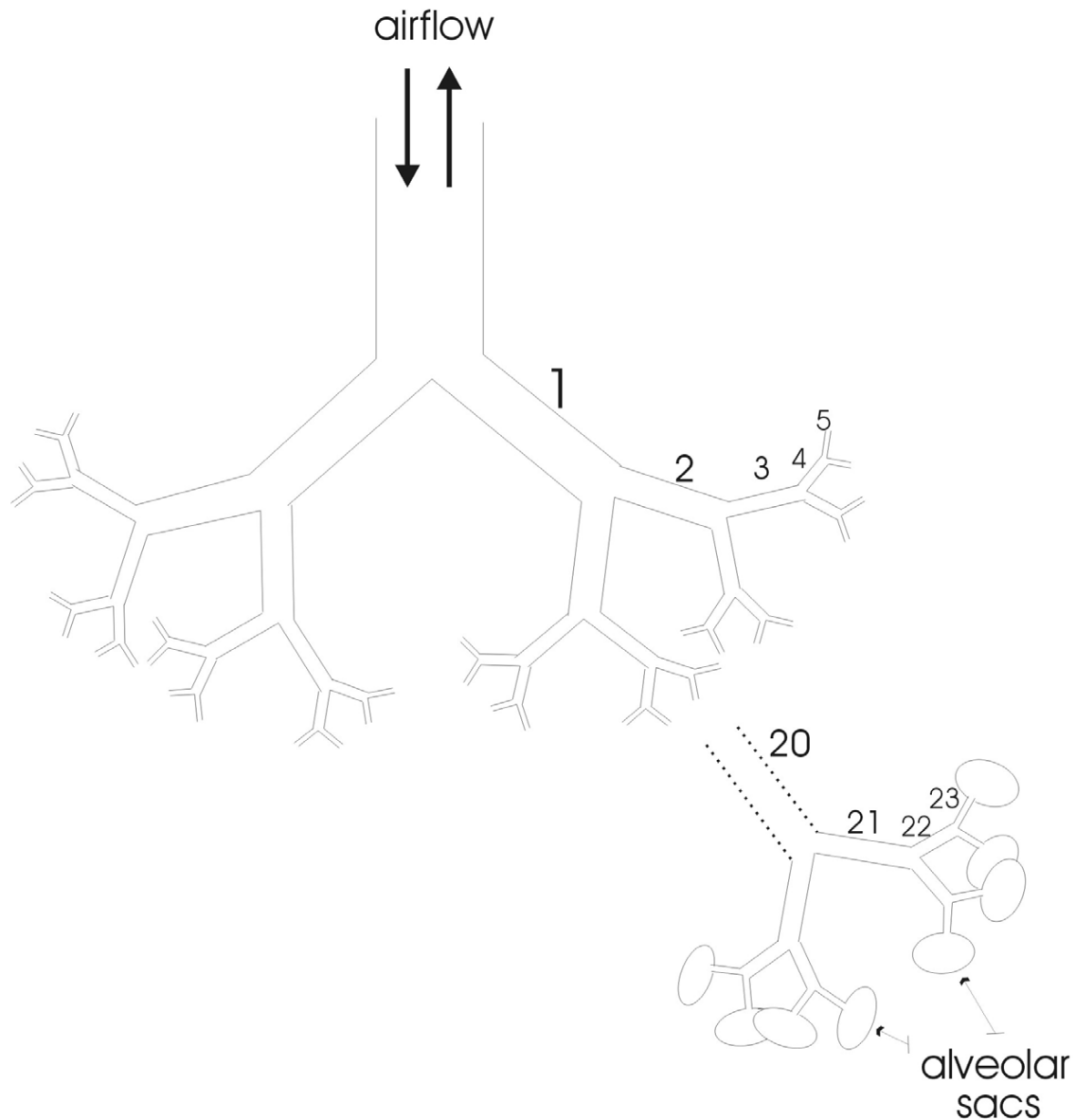
Fig. 3.1 Model of the respiratory tree with trachea, 23 bronchial bifurcations and alveolar sacs.

According to the Constructal Law a fluid tree that performs the oxygenation of blood and removal of carbon dioxide at the lowest flow resistance should exist under the constraints posed by the space allocated to the respiratory process. This fluid tree should be able to promote the easiest access to the external air. Two possibilities exist for accomplishing this purpose: (I) a duct system that ends with an alveolar volume from which the oxygen diffuses to the tissues, where it meets the blood, and in which the carbon dioxide diffuses after being released from the blood, or (II) a unique volume open to the external air, in which the oxygen reaches the blood in the tissues, and removes the carbon dioxide rejected from the blood, only by

diffusion through the internal air.

This second possibility is clearly non-competitive as compared to the first. The access time for a diffusive process between the entrance of the trachea and the alveolar sacs at a distance $L \sim 5 \times 10^{-1}$ m is $t_{diff} = L^2/D \sim 10^4$ s, where $D \sim 2 \times 10^{-5}$ m^2/s is the diffusion coefficient for oxygen in air. The access time for duct flow is of order $t_{flow} = \pi \eta L^2/(D_o^2 \Delta P) \sim 1$ s, where $D_o \sim 10^{-2}$ m is the trachea diameter, $\eta \sim 2 \times 10^{-5}$ Ns/m^2 is air dynamic viscosity, and $\Delta P \sim 1$ Pa is the scale of the average pressure difference. Therefore the channeling of the air from the outside to the alveolar surface enables better performance of the respiratory process.

However, a cavity (or alveolar sac) at the end of the channeling tree must exist, as the oxygenation of the blood occurs by diffusion from air into the tissues. Oxygen diffusion is proportional to the alveolar surface that, in turn, is proportional to the number of bronchioles corresponding to the final level of bifurcation, which is 2^N, N being the number of bifurcation levels. On the other hand, the higher the number of alveolar sacs is, the higher the complexity gets as well as the flow resistance of the duct network. Therefore, the optimum flow structure must emerge from the minimization of the overall resistance, i.e. the duct resistance plus the diffusive resistance.

3.3 Bronchial tree resistance and alveolar resistance

Oxygen and carbon dioxide flow within the respiratory tree (bronchial tree plus alveolar sacs) under several driving forces. So as to evaluate and compare the flow resistances we will express the flow rates in terms of a unique potential. Airflow within the bronchial tree is assumed to be laminar, isothermal and incompressible. As this flow is also adiabatic, i.e. $\Delta s = 0$, conservation of total energy per unit mass that is the sum of internal energy, $u = -P/\rho + Ts + \mu$ (where P is pressure, ρ is density, T is temperature, s is entropy and μ is chemical potential) plus kinetic energy ε, along the respiratory tree, implies:

$$\Delta \mu = \rho^{-1} \Delta P + \Delta \varepsilon \qquad (1)$$

Oxygen and carbon dioxide are assumed to be in equilibrium with the air that flows within the bronchial tree, which means that all gases in the airflow have the same chemical potential and move as a whole between the entrance of the trachea and the alveolar sacs. In this way, the airflow is driven by the gradient of the

chemical potential within the bronchial tree, which in each duct is related to the pressure gradient by Eq. (1) as $\Delta\mu = \rho^{-1}\Delta P$. Hence, by considering the bronchial tree as composed of cylindrical channels and assuming Hagen-Poiseuille flow, the airflow rate is determined by

$$\dot{m}_n = \frac{\pi\rho D_n^4}{128 v L_n}\Delta\mu_{cn} \tag{2}$$

where $\dot{m}_n$ and $\Delta\mu_{cn}$ stand for airflow rate and chemical potential difference between the ends of a channel at the nth bifurcation level, respectively, and v is the air kinematic viscosity. For laminar flow the minimum flow resistance at a bifurcation is achieved if the ratio between consecutive duct diameters is [12,14]:

$$D_n/D_{n-1} = 2^{-1/3} \tag{3}$$

and if the ratio of the respective lengths, L_i , is

$$L_n/L_{n-1} = 2^{-1/3} \tag{4}$$

Eqs. (3) and (4) represent constructal laws that hold for consecutive channels at a bifurcation. They are robust in the sense that hold for any bifurcation angle [12-14] and express the empirical relation known as Murray's law. Taking into account Eqs. (3) and (4), the resistance to laminar flow posed by the nth bronchial tube is

$$r_{cn} = \frac{\Delta\mu_{cn}}{\dot{m}_n} = 2^n\,\frac{128 v L_0}{\pi\rho D_0^4} \tag{5}$$

where D_o and L_o are the diameter and the length of the first tube in the tree i.e. the trachea, respectively.

Each bifurcation implies an additional resistance to airflow. In the derivation of Eq. (2) it has been assumed that pressure has no radial variation along each channel. Such a condition implies that in a bifurcation the variation of the chemical potential is entirely due to the variation in the kinetic energy, as shown in Fig. 3.2 Therefore considering Eq. (1) the airflow rate in a bifurcation may be described by:

$$\dot{m}_n = \frac{\Delta\mu_{bn}}{r_{bn}} = -\frac{\Delta\varepsilon_{bn}}{r_{bn}} \tag{6}$$

where $\Delta\varepsilon_{bn}$ is the variation of the average kinetic energy per unit mass in the bifurcation. Taking into account the velocity (U) profile of cylindrical Hagen-Poiseulle flow, the variation of the kinetic energy per unit mass that flows trough a
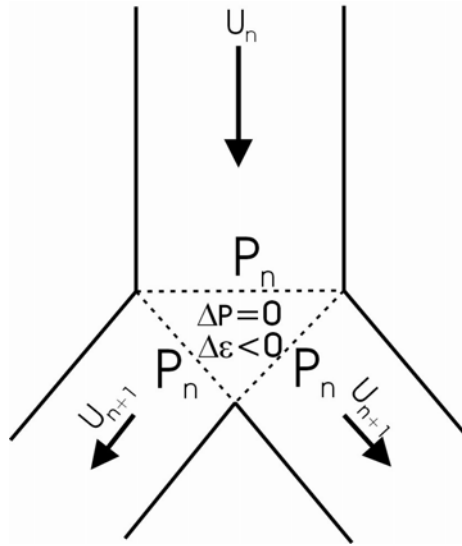
Fig. 3.2 Hagen-Poiseille flow in a bifurcation. The resistance to airflow is due to the variation of the average kinetic energy per unit mass, and proportional to the mass flow rate.

bifurcation is calculated as $\Delta \varepsilon = (\rho / \dot{m}_n)\left(2\int_{n+1}U^3 dA - \int_n U^3 dA\right)$, together with Eqs. (2)-(4), gives the airflow resistance in a bifurcation in the form:

$$r_{bn} = \frac{\dot{m}_0}{8\pi\rho^2 D_0^4} 2^{n/3} \tag{7}$$

where $\dot{m}_0$ represents the airflow rate in the trachea. In this way, with the exception of the channels that connect to the alveolar sacs, every other channel may be viewed as having a Hagen-Poiseulle type resistance given by Eq. (5) plus a resistance at the end due to bifurcation given by Eq. (7).

If $\Delta\mu_n = \Delta\mu_{cn} + \Delta\mu_{bn}$ denotes the total variation of the chemical potential in channels in the nth level of bifurcation ($n=0$, for the trachea), from Eqs (5) and (7) and taking into account that in this level there are 2^n bronchial tubes, we obtain the total resistance of the nth level as

$$r_n = \frac{128\nu L_0}{\pi\rho D_0^4}\left(1 + \frac{\dot{m}_0 2^{-2n/3}}{1024\rho\nu L_0}\right) \tag{8}$$

Then, the overall convective resistance of a tree with trachea ($n=0$) plus (N-1) bifurcation levels is given by

$$R_B = \sum_{n=0}^{N-1} r_n = \frac{128\nu L_0}{\pi\rho D_0^4}\left[N + \frac{\dot{m}_0\left(1 - 2^{-2N/3}\right)}{379\pi\rho\nu L_0}\right] \tag{9}$$

For a normal breathing frequency of 12 times per minute and tidal air of about 0.5 dm³ we conclude that $\dot{m}_0\left(1 - 2^{-2N/3}\right)\!\left(379\pi\rho\nu L_0\right) << 1$, and this term that corresponds to the sum of airflow resistances in the bifurcations may be neglected in Eq. (9).

If $(\phi_{ox})_0$ and ϕ_{ox} denote the average relative concentration of the oxygen in the air at the entrance of the trachea and at the bronchial tree, respectively, the average oxygen current towards the interior of the bronchial tree is

$$\dot{m}_{ox} = \frac{1}{2}\left[(\phi_{ox})_0 - \phi_{ox}\right]\dot{m}_b = \frac{|\Delta\mu_b|}{(R_{ox})_B} \qquad (10)$$

where the subscript ox means oxygen. In Eq. (10) the factor 1/2 arises because either inhaling or exhaling last half of breathing time, $|\Delta\mu_B| = \left|\sum_{n=0}^{N-1}\Delta\mu_N\right|$ is the absolute value of the variation of the chemical potential of the air in the trachea plus the (N-1) levels of bifurcation, and $(R_{ox})_B = 2R_B/\left((\phi_{ox})_0 - \phi_{ox}\right)$ is the resistance to oxygen transport.

However, no such equilibrium conditions exist between the components of the air within the alveolar sacs, because the chemical potential of oxygen in the alveolar tissues is lower than that in the alveolar air, while the chemical potential of carbon dioxide in the tissue is higher than that in the alveolar air. Therefore oxygen diffuses from the alveolar air into the tissues, while carbon dioxide diffuses in the opposite direction. It is assumed that oxygen diffuses at the 2^N alveolar sacs according to Fick's law, consequently the total oxygen current to the alveolar sacs, which are considered to be in a spherical shape with diameter d and total area πd^2 (see Fig. 3), is given by

$$\dot{m}_{ox} = 2^N \int_\pi^0 D_{ox} \frac{(\Delta\rho_{ox})_a \pi d^2 \sin\theta \, d\theta}{2\delta} \qquad (11)$$

where D_{ox} is the oxygen diffusivity, $(\Delta\rho_{ox})_a$ is the difference between the oxygen concentrations at the entrance of the alveolar sac and the alveolar surface, and $\delta = d\sqrt{(1 - \cos\theta)/2}$, (see Fig. 3.3). Taking into account that $(\Delta\rho_{ox})_a = \phi_{ox}\rho(\Delta\mu_{ox})_a/\left(R_g\right)_{ox}T$, where $(R_g)_{ox} = R/M_{ox}$ is the gas constant for oxygen and ϕ_{ox} is the relative concentration of oxygen in the alveolar air, and assuming that
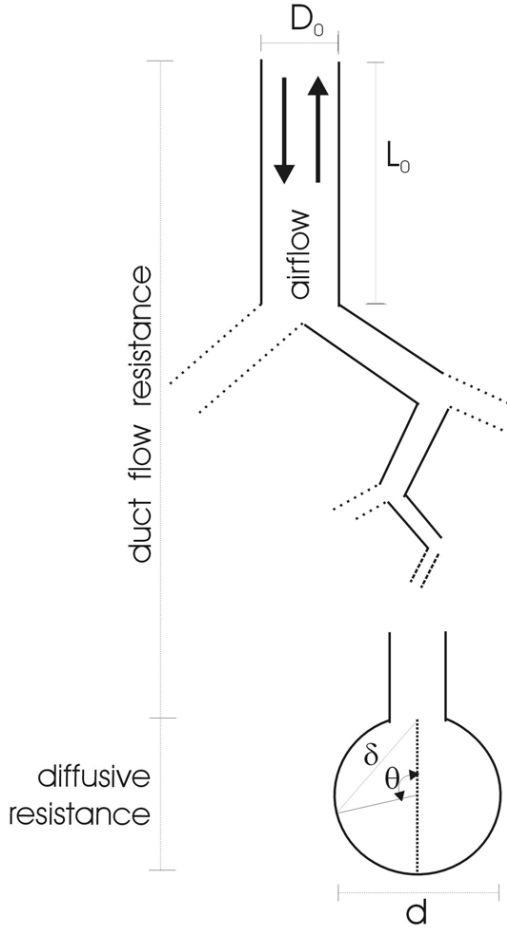
Fig. 3.3 Model of the respiratory tree with a conductive part (bronchioles) and a diffusive space (alveolar sac)

the chemical potential of oxygen does not vary over the alveolar surface, integration of the r.h.s. of Eq. (11) yields:

$$\dot{m}_{ox} = 2^N \frac{2\pi d\rho\phi_{ox}D_{ox}(\Delta\mu_{ox})_a}{(R_g)_{ox}T}$$

(12)

The diameter of the alveolar sac may be determined as the difference between the overall lengths L, of a bronchial tree with infinite bifurcations, which is the limiting length defined by the constructal law, Eq. (4), and that of the actual tree with N bifurcation levels, i.e.

$$d = L - \sum_{i=1}^{N} L_i$$

(13)

The length L_N of a tree with N bifurcations may be determined from Eq. (4) as the length of the trachea plus the lengths of the N consecutive bronchioles is given by the sum of $N + 1$ terms of a geometric series of ratio $2^{-1/3}$ as:

$$\sum_{i=0}^{N} L_i = \frac{1 - 2^{-(N+1)/3}}{1 - 2^{-1/3}} L_0$$

(14)

Therefore, $L = \lim_{N\to\infty} \sum_{i=0}^{N} L_i$, namely $L = 4.85 L_0$. Eqs. (13) and (14) enable us to determine the diameter of the alveolar sac as

$$d = 4.85 \times 2^{-(N+1)/3} L_0$$

(15)

In consequence, Eq. (12) may be written as

$$\dot{m}_{ox} = 7.70\pi L_0\phi_{ox}\rho D_{ox} \frac{2^{2N/3}}{(R_g)_{ox}T}(\Delta\mu_{ox})_a$$

(16)

In this way, the resistance of the Nth level of bifurcation that is the sum of the convective resistance of the last 2^N channels, which is given by $2^{-N}r_{cN}$ (see, Eq. (5)), plus the alveolar diffusive resistance given by Eq. (16), (see also Eq. (10)) is

$$(R_{ox})_N = \frac{128\nu L_0}{\pi\left[(\phi_{ox})_0 - \phi_{ox}\right]\rho D_0^4} + 0.13\left(R_g\right)_{ox}T\frac{2^{-2N/3}}{\pi\phi_{ox}\rho L_0 D_{ox}} \qquad (17)$$

Therefore, if $\Delta\mu_{ox} = (\Delta\mu_{ox})_B + (\Delta\mu_{ox})_N + (\Delta\mu_{ox})_a$ is the total difference between chemical potential of the oxygen in the external air and the oxygen close to the alveolar surface, the total resistance, $R_{ox} = \Delta\mu_{ox}/\dot{m}_{ox}$, posed to oxygen as it moves from the external air into the alveolar surface, which is the sum of the resistance $(R_{ox})_B$, given by Eq. (9), with $(R_{ox})_N$ given by Eq. (17), reads:

$$R_{ox} \cong \frac{256\nu L_0}{\pi D_0^4\left[(\phi_{ox})_0 - \phi_{ox}\right]\rho}(N+1) + \frac{0.13\left(R_g\right)_{ox}T2^{-2N/3}}{\pi L_0 D_{ox}\phi_{ox}\rho} \qquad (18)$$

where the resistances in the bifurcations have been neglected due to the fact that its value is very small as compared to channel resistances. The total resistance is composed of a convective resistance and a diffusive resistance represented by the first and the second terms of the r.h.s of the Eq. (18), respectively.

3.4 Optimisation of the respiratory tree based on the Constructal Law

According to the Constructal Law the flow architectures evolve in time in order to maximize the flow access under the constraints posed to the flow. We believe that, during millions of years of human evolution, the oxygen-access performance of the respiratory tree was optimized naturally, through changes in flow architecture.

In Eq. (18), the convective part of the resistance increases as the number of bifurcations increases, while the diffusive resistance decreases. The number of bifurcations is the free parameter that can be optimized in order to maximize the oxygen access to the alveolar surface or, in other words to minimize the total resistance to oxygen access.

The average value of oxygen relative concentration within the respiratory tree, ϕ_{ox}, may be evaluated from the alveolar air equation in the form: $((\phi_{ox})_o - \phi_{ox})Q - S = 0$, where $(\phi_{ox})_o \sim 1/2(\phi_{air} + \phi_{ox})$ and ϕ_{air} are the oxygen relative concentration at the entrance of the trachea, and in the external air, respectively, Q is the tidal airflow

and S is the rate of oxygen consumption. With $\phi_{air}=0.2095$, $Q\sim6$ dm³/min and $S\sim0.3$ dm³/min [5,11] we obtain $\phi_{ox} \sim 0.1095$.

For L_o we take the sum of the larynx and trachea lengths (first duct), which is typically 15 cm, while the trachea diameter, D_o, is approximately 1.5 cm [10,11). Air and oxygen properties were taken at 36º C, namely $V = 1.7{\times}10^{-5}$ m²/s, $D_{ox} = 2.2{\times}10^{-5}$m²/s, $(R_g)_{ox}=259.8$ J/(kg.K),   The plot of the total resistance of the respiratory tree against the bifurcation level is shown in Fig. 3.4. In can be seen that the minimum is flat and occurs close to $N=23$.

A more accurate value of this minimum is obtained analytically from Eq. (18). The optimum number of bifurcation levels is given by

$$N_{opt} = 2.164\,ln\left[\frac{2.35\times10^{-4}D_0^4\left(R_g\right)_{ox}T}{L_0^2\nu D_{ox}}\left(\frac{(\phi_{ox})_0}{\phi_{ox}}-1\right)\right] \qquad (19)$$

which yields $N_{opt} = 23.4$. As N must be an integer, this means that the optimum number should be 23.
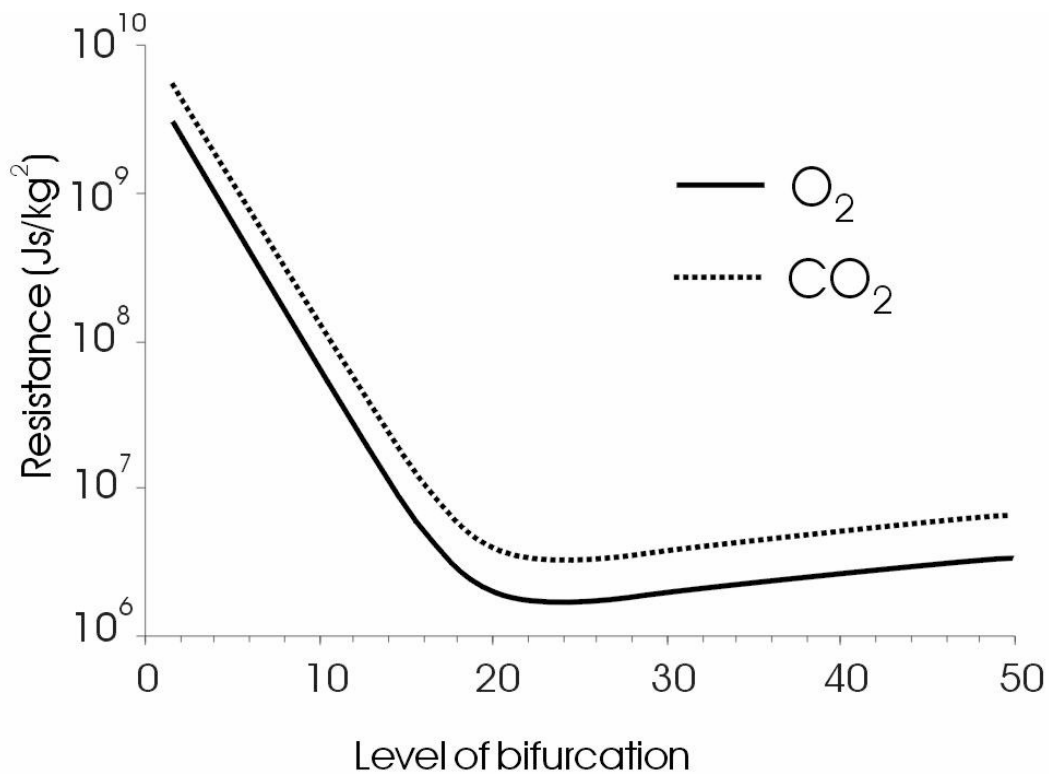

Fig 3.4 Total resistance to oxygen and carbon dioxide transport between the entrance of the trachea and the alveolar surface is plotted as function of the level of bifurcation (n). The minimum resistance both to oxygen access and carbon dioxide removal corresponds to N=23.

In view of the simplifications of the model (mainly the geometry of the bronchial tubes which are assumed to be cylindrical and the geometry of the alveolar sacs which are viewed as spheres, this result is in a very good agreement with the literature, which indicates 23 as the number of bifurcations of the human bronchial tree [4,10].

The respiratory tree can also be optimized for carbon dioxide removal from the alveolar sacs. In this case the correspondent equation to N_{opt} is Eq, (18) with r.h.s multiplied by −1 and the correspondent values of the diffusion coefficient, which is $D_{cd}=1.9 \times 10^{-5} m^2/s$ for carbon dioxide, the gas constant $(R_g)_{cd}=189$ J kg^{-1} K^{-1}, and the value of the average relative concentration of carbon dioxide in the respiratory tree, $\phi_{cd}=0.04$. In the calculation of ϕ_{cd} we used $S=0.24 dm^3/min$ since the respiratory coefficient is close to 0.8 and $(\phi_{cd})_{air} \sim 0.315 \times 10^{-3}$. The plot of the resistance to carbon dioxide removal against bifurcation level is shown in Fig. 4. The minimum resistance, as calculated from Eq. (18), corresponds to $N_{opt} = 23.2$.

We can say that the human respiratory tree, with its 23 bifurcations, is optimized for both oxygen access and carbon dioxide removal. For $N=23$ the resistance to carbon dioxide removal is 4.8×10^6 J s kg^{-2} and higher than the resistance to oxygen access that is 2.60×10^6 J s kg^{-2}.

One of the initial assumptions of this model of respiratory tree was that diffusion can be neglected within the bronchial tree where oxygen is transported in the airflow while diffusion is the main way of oxygen transport in the alveolar sacs. By using Eq. (2) and considering tidal volume of 0.5 dm^3, breathing frequency of 12 times per minute and trachea diameter of 0.015 m, we calculate the average velocity of the airflow, and therefore of the oxygen current, in the last bronchiole before the alveolar sac, which is of order 6mm/s. On the other hand, the average velocity of the diffusive current of oxygen in the alveolar sacs is of order $D_{ox}/2\pi d \sim 1.3$ mm/s. These results are consistent with the initial assumptions of the model. However, as in this idealized model the velocities of the oxygen for convective and diffusive current simply approach each other, in the real respiratory tree we can expect that in some branches they are of the same order, what indicates the possibility of developing alveoli before the end of the bronchial tree as really happens in the human respiratory tree [5].

If the number $N_{opt}=23$ is common to mankind then a constructal rule emerges from Eq. (19): *"the ratio of the square of the trachea diameter to its length is constant and a length characteristic of mankind"*

$$\lambda = \frac{D_0^2}{L_0} = const. = 1.5 \times 10^{-3}\, m \qquad (20)$$

This number has a special relationship with some special features of the space allocated to the respiratory process as we show next. From Eqs. (3) and (4) we can estimate the volume occupied by the bronchial tree, which is the sum of the volumes of the 23 bifurcation levels, as $V_B=23\times(\pi/4)D_o^2L_o$. The total volume of the alveolar sacs is $V=2^{23}(\pi/6)d^3$. We see that $V_B/V<<1$, which means that the volume of the lungs practically corresponds to the volume, V, occupied by the alveolar sacs. The internal area of the alveolar sacs is $A=2^{23}\times\pi d^2$, and therefore $A/V=6/d$. By using the Eqs. (14), (15) which lead to $L = 2^{(N+1)/3}d$, together with Eq. (18) we obtain the following relationship:

$$\frac{D_0^2}{L_0} = 8.63 \frac{AL}{V} \left\{ \frac{v D_{ox}\phi_{ox}}{(R_g)_{ox}T[(\phi_{ox})_0 - \phi_{ox})]} \right\}^{1/2} \qquad (21)$$

The non-dimensional number AL/V, determines the characteristic length $\lambda=D_o^2/L_o$, which determines the number of bifurcations of the respiratory tree by Eq. (19). This constructal law is formulated as follows: *"The alveolar area required for gas exchange, A, the volume allocated to the respiratory system, V, and the length of the respiratory tree, L, which are constraints posed to the respiratory process determine univocally the structure of the lungs, namely the bifurcation level of the bronchial tree."*

From Eq. (14), we obtain $L = 4.85 L_0 = 0.73$m for the total length of the respiratory tree and from Eq. (21) we obtain $d=6V/A=2.86\times10^{-3}$m. Therefore we have the alveolar surface area as $A=2^{23}\pi d^2 =215.5$m^2 and the total alveolar volume $V=2^{23}(\pi/6)d^3 =102.7$dm^3. The alveolar surface area A, is not much far from the values found in literature that fall in the range 100-150m^2. However, the value found for the total alveolar volume is much higher than the average lung capacity ($\sim$7.5 dm^3). This may arise from lung's volume being calculated as the alveolar sacs were fully inflated. Nevertheless, the value found for total alveolar volume suggests that the dimension of the alveolar sacs was somehow overestimated.

3.5 Conclusions

The Constructal Principle that has been successfully employed in engineered systems also proved to be a fundamental tool for the study of flow structures like the respiratory tree. The best oxygen access to the tissues where it reaches the blood is performed by a flow structure composed of ducts with 23 levels of bifurcation. The same structure has been shown to being optimized for carbon dioxide removal as well. At the end of the smallest duct, spaces exist (alveolar sacs) from which the oxygen diffuses to the tissues and in which the carbon dioxide that is removed from the tissues diffuses before reaching the bronchial tree that transports it to the exterior air. The optimized number of bifurcation levels matches the 23 levels that the physiology literature indicates for the human bronchial tree.

In addition, the optimization also predicts the dimension of the alveolar sac, the total alveolar surface area, the total alveolar volume, and the total length of the airways. These values agree, at least in an order of magnitude sense with the values found in the physiology literature. Furthermore, it was shown that the length λ (defined as the ratio between the square of the first airway diameter and its length) is constant for every individual of the same species and related to the characteristics of the space allocated for the respiratory process. This number is univocally determined by a non-dimensional number, AL/V, which involves the characteristics of the space allocated to the respiratory system, namely the total alveolar area, A, the total volume V, and the total length of the airways, L.

In general, we conclude, from Eq. (19), that for every species whose respiratory tree is optimized the same rule must hold, and exhibit the respective characteristic length, λ.

The application of the Constructal Law to the generation of the optimal configuration of the respiratory tree was based on the view that Nature has optimized the living flow structures, in time. The work described in this paper support this view.

Nomenclature

A – alveolar area (m^2)
d – diameter of the alveolus (m)
D – diffusion coefficient (m^2 s)
L – length from the entrance of the trachea to alveolus (m)

$\dot{m}$ – mass flow rate
M – molar mass (kg mol^{-1})
N – total number of bifurcations
P – pressure (Pa)
Q – tidal airflow (dm^3)
r – resistance (J kg^{-2} s^{-1})

R – total resistance (J kg^{-2} s^{-1})

R_g – specific gas constant (J kg^{-1} K^{-1})

s – specific entropy (J kg^{-1} K^{-1})

S – rate of oxygen consumption (kg s^{-1})

t – time (s)

T – temperature (K)

u – specific internal energy (J kg^{-1})

U – velocity (m s^{-1})

V – volume (m^3)

δ – distance from the entrance to the surface of the alveolus (m)

ε – mechanical energy per unit mass (J kg^{-1})

ϕ – relative gas concentration

η – dynamic viscosity (Ns/m^2)

λ – characteristic length (Eq. 20) (m)

μ – chemical potential (J kg^{-1})

ν - kinematic viscosity (m^2 s)

ρ – density (kg m^{-3})

Subscripts

a – relative to alveolus

air – relative to air

B – relative to the bronchial tree

bn – relative to the nth bifurcation.

cd – relative to carbon dioxide

cn – relative to channel of order n

$diff$ – diffusive

i – running index

n – order of bifurcation (o for trachea)

N – relative to the last bifurcation

opt – relative to the optimal value

ox – relative to oxygen

References

[1]A. Bejan, *Shape and Structure, from Engineering to Nature*, (Cambridge University Press, Cambridge, 2000).

[2] J. S. Andrade et al., "Asymmetric Flow in Symmetric Branched Structures," Phys. Rev. Lett., **81**, 4, 926-929 (1998).

[3]B. Mauroy, M. Filoche, J. S. Andrade, and B. Sapoval, "Interplay between geometry and flow distribution in an airway tree," Phys. Rev. Lett., **90**, (14), 926-929 (2003).

[4]V. V. Kulish, J. L. Lage, C. C. W. Hsia, and R. L. Jonhson, "A Porous Medium Model of Alveolar Gas Diffusion," J. Porous Media, **2**, 263-275 (2002).

[5]V. V. Kulish, and J. L. Lage Kulish, "Fundamentals of alveolar diffusion: a new modeling approach," Automedica, **20**, 225-268 (2001).

[6]V. Kulish, J. L. Lage, C. C. W. Hsia, and R. L. Jonhson, "Three-dimensional, Unsteady Simulation of Alveolar Respiration," J. Biomedical Eng., **124**, 609-616 (2002).

[7]K. L. Karau, G. S. Krenz, and C. A. Dawson, "Branching exponent heterogeneity and wall shear stress distribution in vascular trees," Am. J. Physiol. Heart Circ. Physiol., 1256-1263 (2001).

[8]C. G. Phillips, S. R. Kaye, and R. C. Schroter, "A diameter-based reconstruction of the branching pattern of the human bronchial tree I. Description and application," Respiration Physiology **98** (2), 193-217 (1994).

[9] C. G. Phillips, and S. R. Kaye, "Diameter-based analysis of the branching geometry of four mammalian bronchial trees," Respiration Physiology **102** (2-3), 303-316 (1995).

[10] H. Brad et al., Bronchial Anatomy, *Virtual Hospital*, http://www.vh.org/, University of Iwoa, USA (2003).

[11]F. Roberts, "Update in Anaesthesia," Respiratory Physiology **12**, article 11, 1-3 (2000), http://www.nda.ox.ac.uk/wfsa/html/u12/u1211_01.htm#anat

[12]S. Lorente, W. Wechsatol, and A. Bejan, "Three-shaped flow structures designed by minimizing path lengths," Int. J. Heat Mass Transfer, **45**, 3299-3312, (2002).

[13]A. Bejan, L. A. O. Rocha, and S. Lorente, "Thermodynamic optimization of geometry: T- and Y-shaped constructs of fluid streams," S. Int. J. Termal Sciences, **39**, 949-960 (2000).

[14]A. Bejan, I. Dincer, S. Lorente, A. F. Miguel and A. H. Reis, *"Porous and Complex Flow Structures in Modern Technologies"*, ch. 4, Springer-Verlag, N. York (2004).

[15] A. H. Reis, A. F. Miguel and M. Aydin, 2004 "Constructal theory of flow architectures of the lungs" *Medical Physics*, V. **31** (5) pp.1135-1140.

4. Scaling laws of river basins

4.1 Introduction

Flow architectures are ubiquitous in nature. From the planetary circulations to the smallest scales, we can observe a panoply of motions that exhibit organized flow architectures: general atmospheric circulations, oceanic currents, eddies at the synoptic scale, river drainage basins, dendritic crystals, etc. Fluids circulate in all living structures, which exhibit special flow structures such as lungs, kidneys, arteries, and veins in animals and roots, stems, and leaves in plants.

Rivers are large-scale natural flows that play a major role in the shaping of the Earth's surface. River morphology exhibits similarities that are documented extensively in geophysics treatises. For example, Rodríguez-Iturbe and Rinaldo (1997) gave a broad list of allometric and scaling laws involving the geometric parameters of the river channels and of the river basins.

In living structures, heat and mass flow architectures develop with the purpose of dissipating minimum energy, therefore reducing the food or fuel requirement, and making all such systems (animals and "man + machine" species) more "fit," i.e., better survivors.

Constructal theory views the naturally occurring flow structures (their geometric form) as the end result of a process of area to point flow access optimisation with the objective of providing minimal resistance to flow (see Bejan, 2000; Bejan and Lorente, 2004). The Constructal law first put forward by Bejan (1997) stated that "for a finite-size system to persist in time (to live), it must evolve in such a way that it provides easier access to the imposed (global) currents that flow through it."

In the past few decades, extremal hypothesis (e.g. maximum sediment transporting capacity, minimum energy dissipation rate, minimum stream power, minimum Froude number) have been proposed as basis for deducing specific features of river basin morphology and dynamics (see for example the review by Huang and Nanson, 2000). Fractal geometry has also been used to describe river basin morphology (eg., Cieplak et al, 1998; Rodríguez-Iturbe and Rinaldo, 1997). Fractals do not account for dynamics, hence are descriptive rather than predictive.

Because the same morphological laws may be deduced in apparently different contexts some authors have considered fluvial networks and basin geometries as canonical examples of equifinality, which is a concept invented by Beven (2003). Equifinality arises when many different parameter sets are equally good at reproducing an output signal. As pointed out by Savenije (2001), although these models may be based on physical relationships they are not unequivocal, and hence are not fit to be used as predictive models.

What is new with Constructal theory is that it unites geometry with dynamics in such a way that geometry is not assumed in advance but is the end result of an optimisation procedure. Constructal theory is predictive in the sense that it can anticipate the equilibrium flow architecture that develops under existing constraints. In contrast with fractal geometry, self-similarity needs not to be alleged previously, but appears as a result of the constructal optimization of river networks. Moreover, Constructal theory shows that the hypothesis of minimum energy dissipation rate and minimum stream power are corollaries of the Constructal law under particular constraints (Reis, 2006).

The aim of this paper is twofold: to show how the scaling laws of river basins may be anticipated based on Constructal theory, and to present this theory to geomorphologists as a useful tool for the study of the structure of natural flows and landforms. This work adds to a constructal model of erosion put forward by Errera and Bejan (1998), which is able to generate dendrite like patterns of low resistance channels by invoking the Constructal law at each optimization step.

4.2 Scaling laws of river basins

River basins are examples of area-to-point flows. Water is collected from an area and conducted through a network of channels of increasing width up to the river mouth. River networks have long been recognized as being self-similar structures over a range of scales. In general, small streams are tributaries of the next bigger stream in such a way that flow architecture develops from the lowest scale to the highest scale, ω (Fig. 1).

The scaling properties of river networks are summarized in well-known laws. If L_i denotes the average of the length of the streams of order i, Horton's law of stream lengths states that the ratio
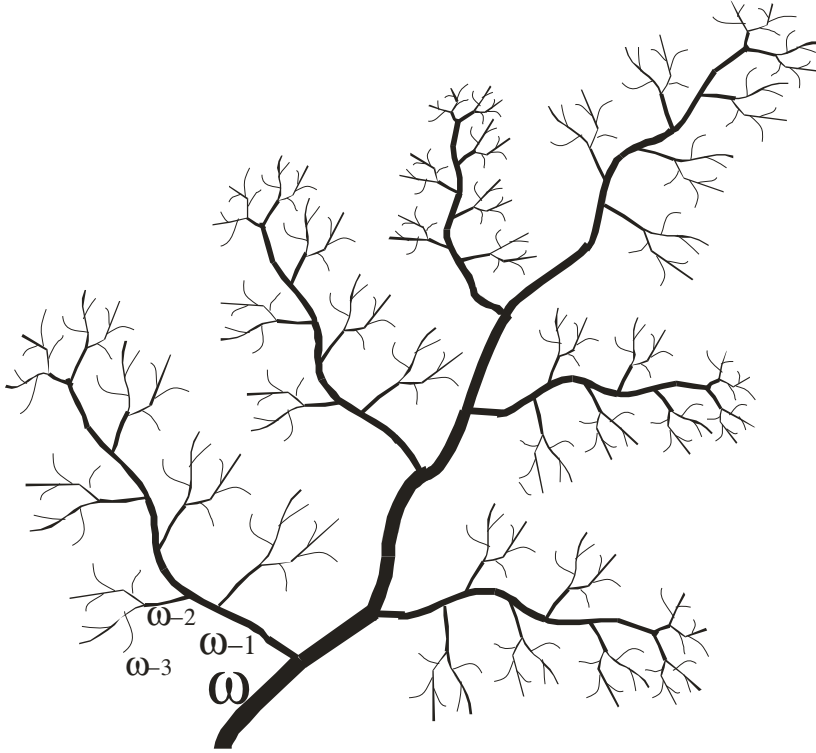
Fig. 4.1 River network with streams up to order ω

$$L_i/L_{i-1} = R_L \tag{1}$$

is a constant (Horton, 1932; see also Raft et al., 2003; Rodríguez-Iturbe and Rinaldo, 1997). Here, the constant R_L is Horton's ratio of channel lengths. On the other hand, if N_i is the number of streams of order i, Horton's law of stream numbers asserts constancy of the ratio

$$N_{i-1}/N_i = R_B \tag{2}$$

where R_B is Horton's bifurcation ratio. In river basins, R_L ranges between 1.5 and 3.5 and is typically 2; while R_B ranges between 3 and 5, typically 4 (Rodríguez-Iturbe and Rinaldo, 1997).

The mainstream length L_ω and the area A_ω of a river basin with streams up to order ω are related through Hack's law (Hack, 1957; see also Rodríguez-Iturbe and Rinaldo, 1997; Schuller et al., 2001):

$$L_\omega = \alpha\left(A_\omega\right)^\beta \tag{3}$$

where $\alpha \sim 1.4$ and $\beta \sim 0.568$ are constants.

If we define a drainage density $D_\omega = L_T / A$ (where L_T is the total length of streams of all orders and A the total drainage area) and a stream frequency $F_s = N_s / A$ (where N_s is the number of streams of all orders) then Melton's law (Melton, 1958; see also Raft et al., 2003; Rodríguez-Iturbe and Rinaldo, 1997) indicates that the following relation holds:

$$F_s = 0.694(D_\omega)^2 \qquad (4)$$

Other scaling laws relating discharge rate with river width, depth, and slope may be found in the book by Rodríguez-Iturbe and Rinaldo (1997).

4.3 River networks as constructal fluid trees

River basins are examples of area-to-point flow, which is a classical topic of Constructal theory. Darcy flow through a porous medium (soil) predominates at the smallest scale. Channelling develops at a higher scale when it becomes more effective than Darcy flow as a transport mechanism. Bejan has addressed this type of flow and, according to the Constructal law, optimized the channel network that minimizes the overall resistance to flow. A detailed treatment can be found in one of his books (Bejan, 2000, Ch. 5). Here, we summarize the optimized area-to-point flow geometry when the conductance of a channel of width W is given by $K = (1/12)W^2$, which corresponds to Hagen-Poiseuille flow between parallel plates.
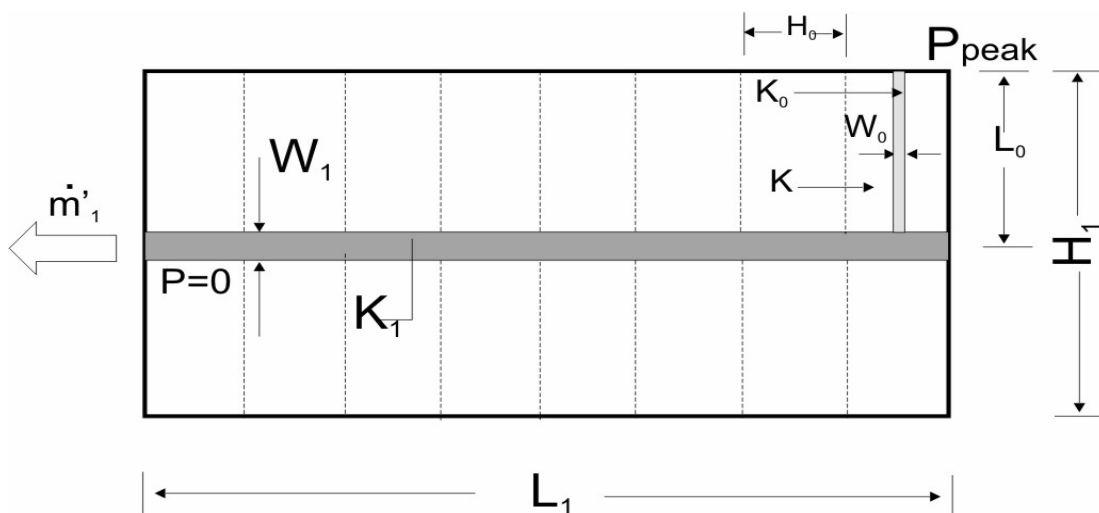

Fig. 4.2 First construct made of elemental areas, $A_o = H_oL_o$. A new channel of higher flow conductance collects flow from the elemental areas.

Table 4.1 The optimized geometry of area-to-point flow (channels with Hagen-Poiseuille flow; Bejan, 2000) ($\hat{K} = K / A_0$; $(\tilde{H}_i, \tilde{L}_i) = (H_i, L_i) / (A_0)^{1/2}$; $\Phi_i = W_i / H_i$)

	$\tilde{H}_i$	$\tilde{L}_i$	n_i
0	$\dfrac{2^{5/6}3^{1/6}\hat{K}^{1/6}}{\Phi_0^{1/2}}$	$\dfrac{\Phi_0^{1/2}}{2^{5/6}3^{1/6}\hat{K}^{1/6}}$	-
1	$\dfrac{2^{1/6}\Phi_0^{1/2}}{3^{1/6}\hat{K}^{1/6}}$	$\dfrac{\Phi_1^{3/2}}{2^{3/2}\hat{K}^{1/2}}$	$\dfrac{\Phi_1^{3/2}\Phi_0^{1/2}}{2^{4/3}3^{1/6}\hat{K}^{2/3}}$
2	$\dfrac{\Phi_1^{3/2}}{2^{1/2}\hat{K}^{1/2}}$	$\dfrac{3^{1/6}(\Phi_2\Phi_1)^{3/2}}{2^{5/3}\Phi_0^{1/2}\hat{K}^{5/6}}$	$\dfrac{3^{1/3}(\Phi_2\Phi_1)^{3/2}}{2^{5/6}\Phi_0\hat{K}^{2/3}}$
3	$\dfrac{3^{1/6}(\Phi_2\Phi_1)^{3/2}}{2^{2/3}\Phi_0^{1/2}\hat{K}^{5/6}}$	$\dfrac{3^{1/3}(\Phi_3\Phi_2\Phi_1)^{3/2}}{2^{4/3}\Phi_0\hat{K}^{7/6}}$	$\dfrac{2^{1/6}3^{1/3}(\Phi_3\Phi_2)^{3/2}}{\Phi_0\hat{K}^{2/3}}$
4	$\dfrac{3^{2/3}(\Phi_3\Phi_2\Phi_1)^{3/2}}{2^{1/3}\Phi_0\hat{K}^{7/6}}$	$\dfrac{3^{1/2}(\Phi_4\Phi_3\Phi_2\Phi_1)^{3/2}}{2^{1/2}\Phi_0^{3/2}\hat{K}^{9/6}}$	$\dfrac{2^{7/6}3^{2/3}(\Phi_4\Phi_3)^{3/2}}{\Phi_0\hat{K}^{2/3}}$

If H_i and L_i represent the dimensions of the area $A_i = H_i \times L_i$ allocated to each stream of order i, the peak pressure $P_{peak,1}$ at the farthest corner of the first construct (see Fig. 2) is given by (Bejan, 2000)

$$\frac{P_{peak,1}}{\dot{m}_1'\nu / K} = \frac{1}{4\tilde{K}_0\Phi_0}\frac{H_1}{L_1} + \frac{1}{2\tilde{K}_1\Phi_1}\frac{L_1}{H_1} \tag{5}$$

where $\dot{m}_1'$ represents total mass flow rate, ν is viscosity of water, $\tilde{K}_i = K_i / K$, and $\Phi_i = W_i / H_i$. Minimizing the flow resistance over the first construct is equivalent to minimize the peak pressure, $P_{peak,1}$ in Eq. (5). Each new construct A_i contains n_i constructs of area A_{i-1}, the flow of which is collected by a new high conductance channel. The maximum pressure difference sustained by A_i is equal to the sum of the pressure difference across the already optimized constituent A_{i-1} that occupies the farthest corner of A_i, and the pressure drop along the central channel of A_i (Bejan, 2000):

$$P_{peak,i} = P_{peak, i-1} + \dot{m}_i'\nu \frac{L_i}{2K_iW_i} \tag{6}$$

With n_i representing the number of streams of order i that are tributaries of each stream of order $i+1$, the optimized values of stream channels up to order 4 are shown in Table 4.1.

Table 4.2 The jointly optimised network parameters (minimization of the overall resistance to flow and optimisation of void stream area allocation)

	$\widetilde{L}_i$	n_i
0	$0.47\left(\Phi_0\hat{K}^{-1/3}\right)^{1/2}$	–
1	$0.36\left(\Phi_0\hat{K}^{-1/3}\right)^{3/2}$	$0.33\left(\Phi_0\hat{K}^{-1/3}\right)^2$
2	$0.30\left(\Phi_0\hat{K}^{-1/3}\right)^{5/2}$	$0.81\left(\Phi_0\hat{K}^{-1/3}\right)^2$
3	$0.31\left(\Phi_0\hat{K}^{-1/3}\right)^{7/2}$	$0.88\left(\Phi_0\hat{K}^{-1/3}\right)^2$
4	$0.41\left(\Phi_0\hat{K}^{-1/3}\right)^{9/2}$	$2.00\left(\Phi_0\hat{K}^{-1/3}\right)^2$

Table 4.3 Constructal Horton ratios of stream lengths, R_L

$\widetilde{L}_1/\widetilde{L}_0$	$\widetilde{L}_2/\widetilde{L}_1$	$\widetilde{L}_3/\widetilde{L}_2$	$\widetilde{L}_4/\widetilde{L}_3$
$0.76\Phi_0\hat{K}^{-\frac{1}{3}}$	$0.85\Phi_0\hat{K}^{-\frac{1}{3}}$	$1.04\Phi_0\hat{K}^{-\frac{1}{3}}$	$1.33\Phi_0\hat{K}^{-\frac{1}{3}}$

A second kind of constructal optimization is performed with respect to the optimal distribution of the total void volume corresponding to the channels. The optimal allocation of channel volume is such that it minimizes the global void volume under both constant basin area and flow resistance (see Bejan and Lorente, 2004). The void-allocation (channel) optimization provides the following additional relationships (Bejan, 2000, pp. 91-94):

$$\Phi_1 = \Phi_0 \quad ; \quad \Phi_2 = (6/7)\Phi_0 \quad ; \quad \Phi_3 = (60/77)\Phi_0 \quad ; \quad \Phi_4 = (8/11)\Phi_0 \quad (7)$$

With Eq. (7), $\widetilde{L}_i$ and n_i may be rewritten in the forms shown in Table 2. Both $\widetilde{L}_i$ and n_i depend uniquely on $\Phi_0\hat{K}^{-1/3}$ which, in turn, is the product of two terms: (i) Φ_0 that represents the ratio of the area of the smallest (first order) channel to the area of the porous layer that feeds it and (ii) the dimensionless conductance $\hat{K}$ raised to the power (– 1/3). As none of these parameters depend upon the particular geometry of the layer, we conclude that despite the relationships of Tables 4.1 and 4.2 being derived from constructs of regular geometry as that of Fig. 4.2, the relationships in Table 4.2 are applicable to any hierarchical stream network irrespective to its particular geometry.

Table 4.4 Dimensionless area of constructal river basins up to order 4

$\widetilde{A}_0$	$\widetilde{A}_1$	$\widetilde{A}_2$	$\widetilde{A}_3$	$\widetilde{A}_4$
1	$0.33\left(\Phi_0\hat{K}^{-1/3}\right)^2$	$0.21\left(\Phi_0\hat{K}^{-1/3}\right)^4$	$0.19\left(\Phi_0\hat{K}^{-1/3}\right)^6$	$0.37\left(\Phi_0\hat{K}^{-1/3}\right)^8$

Channel hierarchy is understood in the Hortonian sense, i.e., all streams of order i are tributaries of streams of order i+1.

River basins are examples of area-to-point flows that approach the Hortonian hierarchy; therefore, the constructal rules defined in Table 2 for stream networks up to order 4 must hold, at least approximately. For example, with the use of Table 2, the ratios of the lengths of consecutive streams are given in Table 3. We see that the ratio of the characteristic lengths of streams of consecutive order $\widetilde{L}_{i-1}/\widetilde{L}_i \sim \Phi_0\hat{K}^{-1/3}$ is practically constant as required by Horton's law of stream lengths (Eq. 1).

To check if the constructal relations in Table 2 match Horton's law of stream numbers (Eq. 2), we calculate the number N_i of streams up to order i, which is given by

$$N_i = n_i \times n_{i-1} \times n_{i-2} \times ... \times n_1 \tag{8}$$

where n_j is the number of streams of order j that are tributaries of each stream of order j+1. Taking into account Eq. 8, the ratio of the number of streams up to order i to the number of streams up to order i-1 is given by

$$N_i/N_{i-1} = n_i \tag{9}$$

The ratios n_i are shown in Table 4.2. We conclude that these ratios are almost of the same order, i.e., $N_i/N_{i+1} \sim \left(\Phi_0\hat{K}^{-1/3}\right)^2$; therefore matching Horton's law of stream numbers, closely. Recalling that the ratio of stream lengths is $\widetilde{L}_{i+1}/\widetilde{L}_i \sim \Phi_0\hat{K}^{-1/3}$, we conclude that

$$N_i/N_{i+1} \sim \left(\widetilde{L}_{i+1}/\widetilde{L}_i\right)^2 \tag{10}$$

i.e., the ratio of stream numbers is of the order of the square of the ratio of stream lengths. As stated in the introduction, in real river basins $L_i/L_{i-1} = R_L$ ranges between 1.5 and 3.5, and is typically 2, while $n_{i-1}/n_i = R_B$ ranges between 3 and 5, typically 4 (Raft et al., 2003; Rodríguez-Iturbe and Rinaldo, 1997), i.e., the constructal rule evinced by Eq. 10 is closely verified for the real river basins.

Table 4.5 Constructal Hack's exponent β for river basins up to order 4

$\tilde{L}_1 \sim A_1^{0.75}$	$\tilde{L}_2 \sim A_2^{0.62}$	$\tilde{L}_3 \sim A_3^{0.58}$	$\tilde{L}_4 \sim A_4^{0.56}$
$\beta = 0.75$	$\beta = 0.63$	$\beta = 0.58$	$\beta = 0.56$

Next we are going to show that Hack's law (Eq. 3) also follows from the constructal relationships of Tables 4.1 and 4.2. Noting that $A_i = H_i L_i$ and using Table 4.1 and Eq. (7), we obtain the sub basin areas shown in Table 4.4. The constructal relationships between mainstream length L_ω and the area A_ω of a river basin with streams up to order ω is determined by using Table 4.4 together with Table 4.2 and is shown in Table 4.5. Gray (1961) found $\beta \sim 0.568$ while Muller (1973) reported that $\beta \sim 0.6$ for river basins < 8000 mi² (1 mile = 1609.3 m), $\beta \sim 0.5$ for basins between 8000 and 100,000 mi², and $\beta \sim 0.47$ for basins > 100,000 mi² (see also Schuller et al., 2001).

The constructal rule for the exponent β is the following:

$$\beta_\omega = \frac{2\omega + 1}{4\omega} \tag{11}$$

We see from Eq. 11 that as the order of the river basin increases, β approaches 0.5 in good agreement with Muller's findings for actual river basins.

In order to check Melton's law, first we calculate the drainage density D_ω as

$$D_\omega = \sum_{i=1}^{\omega} n_i \tilde{L}_i \Big/ \tilde{H}_\omega \tilde{L}_\omega \tag{12}$$

and the stream frequency as

$$F_\omega = \sum_{i=1}^{\omega} N_i \Big/ \tilde{H}_\omega \tilde{L}_\omega \tag{13}$$

By using Tables 1 and 2 and with the help of Eq. (8) we obtain:

$$D_4 = 0.18\left(\Phi_0 \hat{K}^{-1/3}\right) + 0.14\left(\Phi_0 \hat{K}^{-1/3}\right)^{-0.5} + 0.35\left(\Phi_0 \hat{K}^{-1/3}\right)^{-1.5} + 0.44\left(\Phi_0 \hat{K}^{-1/3}\right)^{-2.5} \tag{14}$$

and

$$F_4 = 1 + 0.38\left(\Phi_0 \hat{K}^{-1/3}\right)^{-2} + 1.16\left(\Phi_0 \hat{K}^{-1/3}\right)^{-4} + 1.42\left(\Phi_0 \hat{K}^{-1/3}\right)^{-6} \tag{15}$$

We note that the drainage density of a stream of order 0 is $(L_0/H_0)^{1/2}$, while the stream frequency is 1, which is the lowest limit.
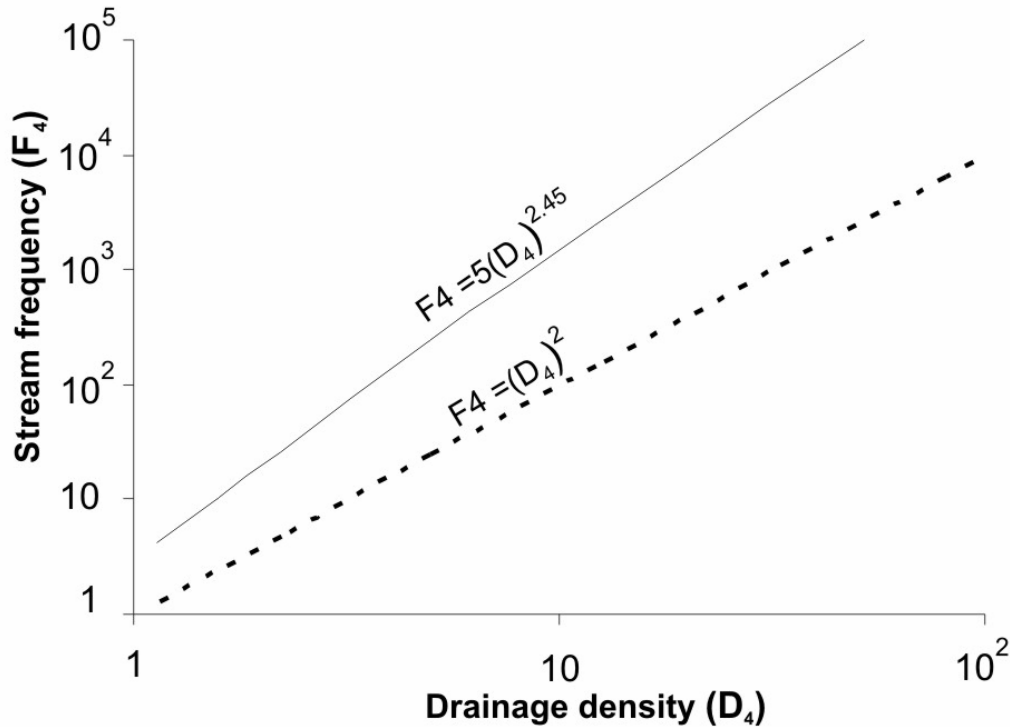
Fig. 4.3 For a river basin of order 4, the constructal relationships indicate that steam frequency is proportional to drainage density raised to a power of 2.45, which is close to 2 (Melton's law).

The variation of F_4 with D_4 is shown in Fig. 4.3. We see that the constructal relations in Eqs. 14 and 15 follow Melton's law quite approximately in the range $1 < D_4 < 10^2$, i.e., F_4 is proportional to D_4 raised to the power 2.45.

The scaling laws of river basins evince the organized flow architectures that result from the underlying struggle for better performance, by reducing the overall resistance in order to drain water from the basins the fastest (Constructal law) and the best uniformly distributed all over the basin area.

4.   Conclusions

Despite only basins with streams up to order 4 having been considered in this paper, we believe that the conclusions do extend to higher order river basins.

The scaling laws of geometric features of river basins can be anticipated based on Constructal theory, which views the pathways by which drainage networks develop in a basin not as the result of chance but as flow architectures that originate naturally as the result of minimization of the overall resistance to flow (Constructal law).

The ratio of constructal lengths of consecutive streams match Horton's law for the same ratio, while the same occurs with the number of consecutive streams that match Horton's law of ratios of consecutive stream numbers.

Hack's law is also correctly anticipated by the constructal relations that provide Hack's exponent accurately.

Melton's law is anticipated approximately by the constructal relationships that indicate 2.45 instead of 2 for Melton's exponent. However, the difficulty to calculate correctly the drainage density and the stream frequency from field data indicates that some uncertainty must be assigned to Melton's exponent.

These results add to many other examples of complex flows, either from engineering (e.g., Bejan 2000; Bejan et al., 2004) or from animate structures (e.g. Bejan, 2000; Reis et al., 2004), in which the Constructal law proved to play a fundamental role.

NOMENCLATURE

A – Area (m^2)

D – Drainage density (m^{-1})

F – Stream frequency (m^{-2})

H – Width of a construct (m)

$\hat{K}$, $\widetilde{K}$ – Dimensionless channel flow conductance

L – Stream length (m)

$\widetilde{L}$ – Dimensionless length (construct, channel)

N_i – Total number of streams of order i

n – Number of streams that are tributaries of each stream of the next order

R_B – Horton's bifurcation ratio

R_L – Horton's ratio of stream lengths

W – Channel width (m)

Φ – Aspect ratio, W/H

Subscripts

i – Order of a stream

s – Relative to stream

T – Total

ω – Order of the river basin

o – Relative to the elemental construct

References

Bejan, A., 1997. Advanced Engineering Thermodynamics. 2nd Ed. Wiley, New York, Ch. 13.
Bejan, A., 2000. Shape and Structure, from Engineering to Nature. Cambridge University Press, Cambridge, UK.
Bejan, A., Lorente, S., 2004. The Constructal law and the thermodynamics of flow systems with configuration. Int. J. Heat and Mass Transfer 47, 3203-3214.
Bejan, A., Dincer, I., Lorente, S., Miguel, A.F., Reis, A.H., 2004. Porous and Complex Flow Structures in Modern Technologies. Springer-Verlag, New York.

Beven K., 1993. Prophesy, reality and uncertainty in distributed hydrological modelling. Advances in Water Resources 16, 41-51.

Cieplak, M., Giacometti, A., Maritan, A., Rinaldo, A., Rodriguez-Iturbe, I., Banavar, J. R., 1998. Models of Fractal River Basins. J. of Statistical Physics 91, 1-15.

Errera, M.R. and Bejan, A., 1998. Deterministic tree networks for river drainage basins. Fractals 6, 245-261.

Gray, D.M., 1961. Interrelationship of watershed characteristics. J. of Geophysical Research 66, 1215–1223.

Hack, J.T., 1957. Studies of longitudinal profiles in Virginia and Maryland. USGS Professional Papers 294-B, Washington DC, pp. 46–97.

Horton, R.E., 1932. Drainage basin characteristics. EOS Trans. AGU 13, 350-361.

Huang, H.Q., Nanson, G.C., 2000. Hydraulic geometry and maximum flow efficiency as products of the Principle of Least Action. Earth Surface Processes and Landforms 25, 1-16.

Melton, M.A, 1958. Correlation structure of morphometric properties of drainage systems and their controlling agents. J. of Geology 66, 35-56.

Muller, J.E., 1973. Re-evaluation of the relationship of master streams and drainage basins: Reply. Geological Society of America Bulletin 84, 3127–3130.

Raft, D.A., Smith, J.L., Trlica, M.J., 2003. Statistical descriptions of channel networks and their shapes on non-vegetated hillslopes in Kemmerer, Wyoming. Hydrol. Processes 17, 1887-1897.

Reis, A.H., 2006. Constructal Theory: From Engineering to Physics, or How Flow Systems Develop Shape and Structure.

Reis, A. H.. 2006 "Constructal view of scaling laws of river basins", *Geomorphology*, Vol. **78**, 201-206.

Reis, A.H., Miguel, A.F., Aydin, M., 2004. Constructal theory of flow architectures of the lungs. Medical Physics 31 (5), 1135-1140.

Rodríguez-Iturbe, I., Rinaldo A., 1997. Fractal River Basins. Cambridge University Press, New York.

5. Scaling laws of street networks – the dynamics behind geometry

5.1 Introduction

Cities are very complex systems that have developed in time under the influence of multiple factors (politics, social structure, defence, trade, etc). Even though the relative weights of these factors seem to vary very much from city to city, some features have been noticed that are common to all cities. For example, it has been verified that cities possess self-similar structures that repeat over a hierarchy of scales [1, 2]. This provided the basis for many authors to claim that many aspects of cities allow a fractal description [3 - 9]. This observation, however does not explain why cities do share this architectural similarity. Idealists would claim that, as cities are complex man-made systems this common aspect springs from the congenital ideas of beauty and harmony shared by mankind. On the other hand, constructal theory considers that dynamics is behind geometry, such that geometry evolves just as the envelope of underlying dynamic processes. The Constructal law first put forward by Bejan [10] states that "for a finite-size system to persist in time (to live), it must evolve in such a way that it provides easier access to the imposed (global) currents that flow through it."

Cities are living systems in the sense that they have proper "metabolism" driven by the activities of their inhabitants, are open to flows of goods and people, and evolve in time. Lanes, roads, streets, avenues constitute the vascular network of cities. As with every living system, city networks have evolved in time such as to provide easier and easier access to flows of goods and people. Street networks of today's cities tell the old story of the dynamics of the past. From the ancient to the newest district we can observe the development of streets of decreasing flow resistance, or, said another way increasing access for people and goods [11]. The street networks of the old parts of today's cities are fossils that testify the past dynamics of the city.

5.2 Fractal description

Hierarchically organized structures, in the sense that a structure of dimension x is repeated at the scales rx, r^2x, r^3x, ..., where r is a scale factor, have

been noticed in most of today's cities. Structure self-similarity at various scales indicates that such structures allow fractal description if some property ϕ of the self-similar structure obeys the relationship

$$\phi(rx) = r^m \phi(x) \tag{1}$$

where m is the fractal dimension. Examples of repeated self-similar structures are some patterns of street networks that look the same at various scales.

In a city the number of pieces (e.g. streets) N(X) of size X seems to follow an "inverse-power distribution law" of the type

$$N(X) = CX^{-m} \tag{2}$$

where C is a constant and $1 \leq m \leq 2$ [12]. Therefore, if X_o is the dimension of the city, by using eq. (1), the number of pieces of dimension $X_n = X_0 r^{-n}$ is given by

$$N(X_n) = CX_0 r^{-nm} \tag{3}$$

The rule conveyed by eq. (3) is a distribution of geometric patterns solely, and does not make clear why city structures organize in such a way. We sustain that the reasons for such a particular distribution grounds on the underlying city dynamics.

5.3 Flow structures in a city

Cities have their own metabolism that consists of people's everyday activities. People exchange and consume goods and services in cities and, because cities are open systems, with the rest of the world. The various flows that cross the cities distribute people and goods to the proper places for daily activities.

By walking or by using means of transportation, people and goods flow through the inner vascular system that covers the city territory. Each of these means of transportation uses a proper channel to move in. People's movements starts being unorganized (erratic when if we consider a group of individuals) showing the characteristics of a diffusive flow, then becomes progressively organized (more and more people moving in the same ways) as people move into the larger ways. Public transportation exists because individuals agree in moving together in some direction. It is also a way of saving exergy and time. The speed of transportation increases as individuals proceed from home to the larger ways (Fig. 5.1)
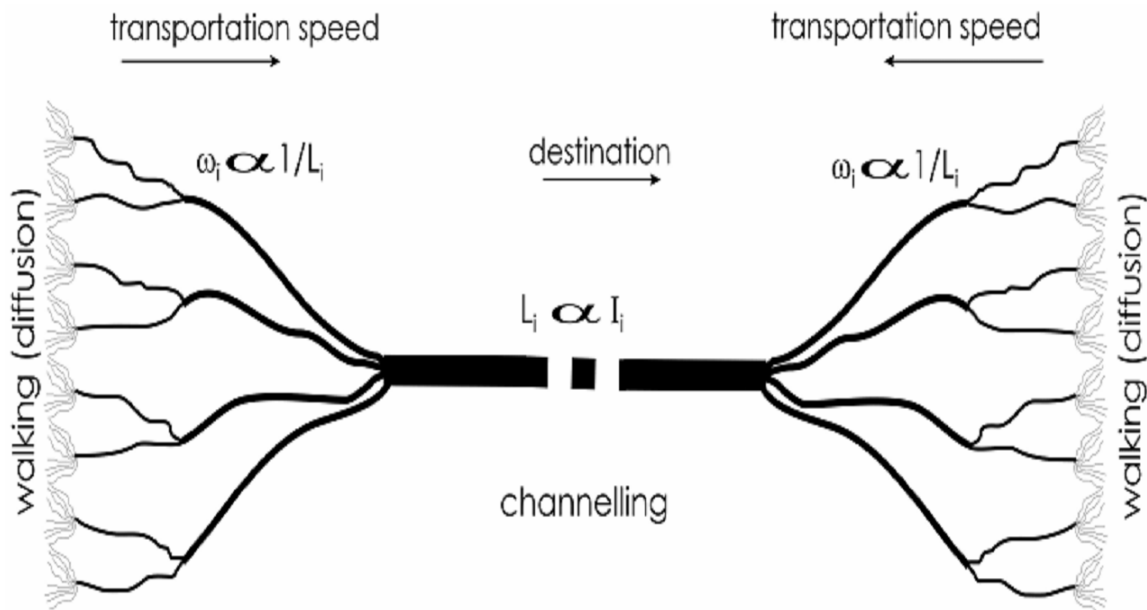
Fig. 5.1 Area to point and point to area flows. Individuals move from one area to another by using successively faster means transportation first, this rule being inverted as they approach the area of destination.

In some aspects, modelling flows of people is not the same as modelling flows of inanimate fluids. In fact, fluids are ensembles of particles that act in a purely mechanistic way, i.e. under the action of known external forces. In the later case, the Navier-Stokes equation, which equates driving against dissipation (brake) forces, together with boundary and initial conditions, is sufficient to predict the flow. However, in flows of people, the individuals are not only subjected to external forces as fluids are, but as living systems experience also "internal" forces, most known as desire, decision, etc. Then, how to physically model such biased forces? In fact we cannot, but instead we can model their effect by accounting for the resulting entropy generation rate. In this way we will be able to precisely define the resistance to flow.

For example, consider a street of width W, with spatial concentration of cars, σ (cars/m²), that flow with an average velocity v (m/s). If some car proceeds with a positive velocity difference of order Δv with respect to the next one, then its driver has to slow down on the same Δv in order not to hit that car. Therefore, the exergy lost is the process is $\varepsilon = -mv(\Delta v)$, to which corresponds the entropy generation, $s_{gen} = -\varepsilon/T$, where T is ambient temperature (Guy-Stodola theorem).
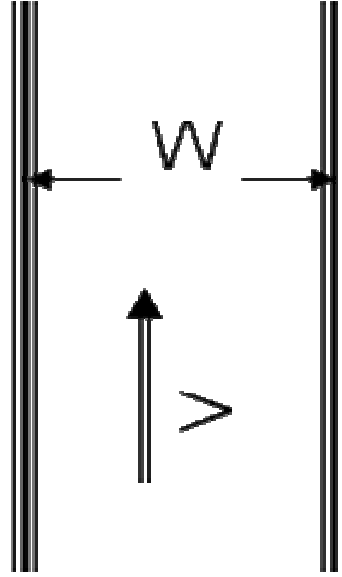
Fig. 5.2 Flow at average speed v in a street of width W.

Let θ_i be the fraction of the number of cars in the control area W×L, with velocity difference Δv_i with respect to the next car, and let λ be the safety distance between successive cars (see Fig. 5.2).

Then, the total number of decelerations per second in the control area is given by $\sigma\sum_i \theta_i(\Delta v_i)W\,L/\lambda$, while the total power (exergy/s) lost $\dot{E}_i$ is given by

$$\dot{E} = \sigma\sum_i \theta_i(\Delta v_i)W(L/\lambda)m_i v(\Delta v_i) \tag{4}$$

where v is the average speed of the cars. According the Guy-Stodola theorem the entropy generation rate $\dot{S}_{gen}$ is given by:

$$T\dot{S}_{gen} = -\dot{E} \tag{5}$$

Then, eq. (5) enables us to define the flow resistance, R, as

$$R = T\dot{S}_{gen}\big/I^2 \tag{6}$$

where I represents the car (people) flow rate in the street, which is given by

$$I = \sigma v W \tag{7}$$

According to eq. (6) the resistance to flow is proportional to the entropy generation rate per car (people) flow rate. Therefore, whatever the nature of the potential difference ΔV that drives the flow is, the end result is always exergy dissipation, $(\Delta V)I$, which balances entropy generation

$$\Delta V = - T\dot{S}_{gen}\big/I \tag{8}$$

By considering the eqs. (4-7) the flow resistance reads

$$R = \sum_i \theta_i m_i (\Delta v_i)^2 L \big/ (\sigma\lambda v W) \tag{9}$$

It is commonly observed that the wider the street, the higher the average velocity of what flows in. We assume, as a first approach, that the average velocity is proportional to street width, i.e. $v = kW$, and therefore eq. (9) reads

$$R = \sum_i \theta_i m_i (\Delta v_i)^2 L \big/ \left(\sigma\lambda k W^2\right) \tag{10}$$

The group $v = \sum_i \theta_i m_i (\Delta v_i)^2 \big/ \overline{m}\left(\sigma\lambda^2 k\right)$, where m represents average mass of cars (people) has dimension of viscosity and characterizes the "fluid" that flows in the street. Then, then by inserting v in eq. (10) it turns into

$$R/L = v\lambda\big/W^2 \ , \tag{11}$$

which indicates that the flow resistivity is directly proportional to the "viscosity" of what flows and inversely proportional to street width. The resistibility of the "street flows" shows the same dependence on channel width W as with "Hagen-Poiseuille flow" between parallel plates. This feature enables us to use the results of constructal optimizations previously carried out for river basins [13, 14]. In fact, Chen and Zhou [15] had already noticed that the city scaling laws take the form of known laws of geomorphology, namely of river basins. What we show next is that as with the river basins also the scaling laws of city networks emerge from the underlying dynamics.

5.4 City networks and fractal dimension

Bejan (2000), optimized flow trees for area-to-point flows, of resistivity $R/L \propto 1/W^2$, in two ways: (i) by minimizing global resistances under constant flow rate and "drainage area"; (ii) by minimizing the volume (area) allocated to channels (streets) in the tree subject to fixed global resistances and "drainage area". Reis [14] showed that Bejan's relations anticipate known scaling laws of river basins (Fig. 5.3).
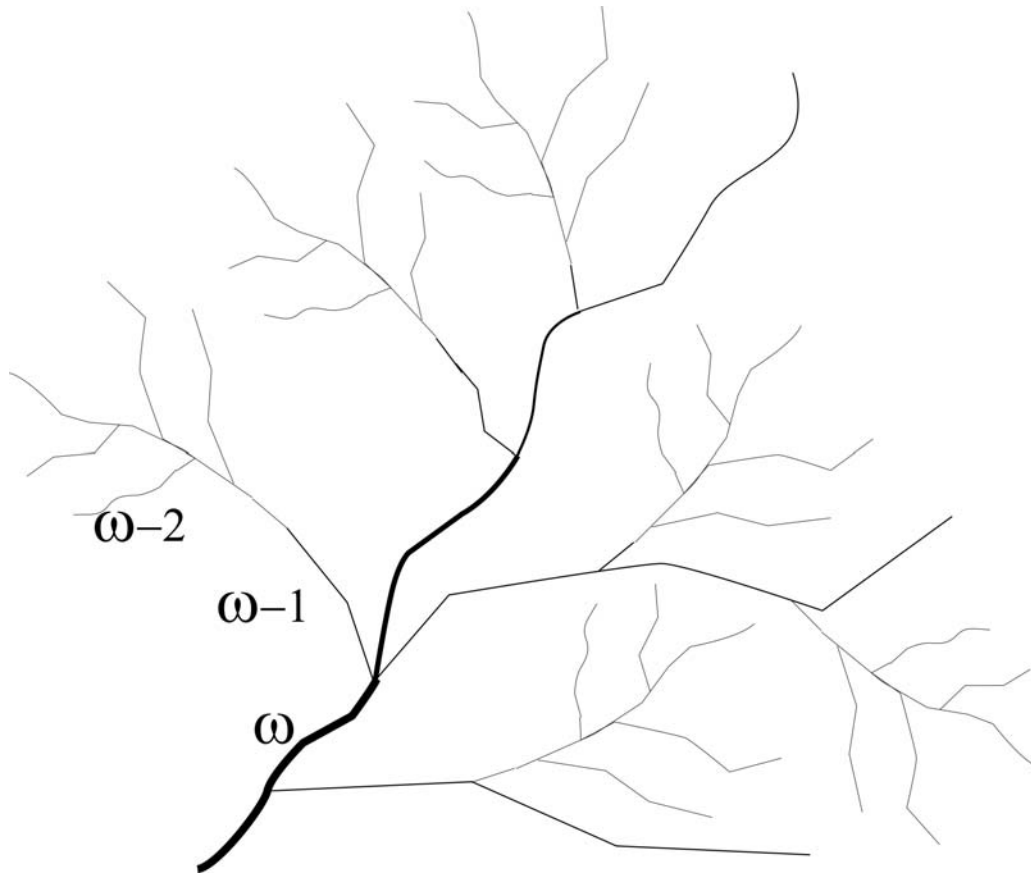
Fig. 5.3 River basin with streams up to order ω. Streams of order $\omega - n - 1$ are tributaries of streams of order $\omega - n$.

One of such laws tells us that the ratio of the average lengths of streams of consecutive hierarchical order is constant, i.e.

$$\frac{L_n}{L_{n+1}} = R_L \tag{12}$$

where $R_L \sim 2$, while the same happens with the average number of streams of consecutive hierarchical order, i.e.

$$\frac{N_{n+1}}{N_n} = R_N \tag{13}$$

which is also a constant, $R_N \sim 4$ (see Fig. 5.4). Reis [14] showed that despite the relationships (12) and (13) have been derived from constructs of regular geometry as those of Fig. 5.4, they hold for any hierarchical stream network irrespective to its particular geometry. Moreover, relationships (12) and (13) imply that they are self-similar in its range of validity (see also Fig.2).
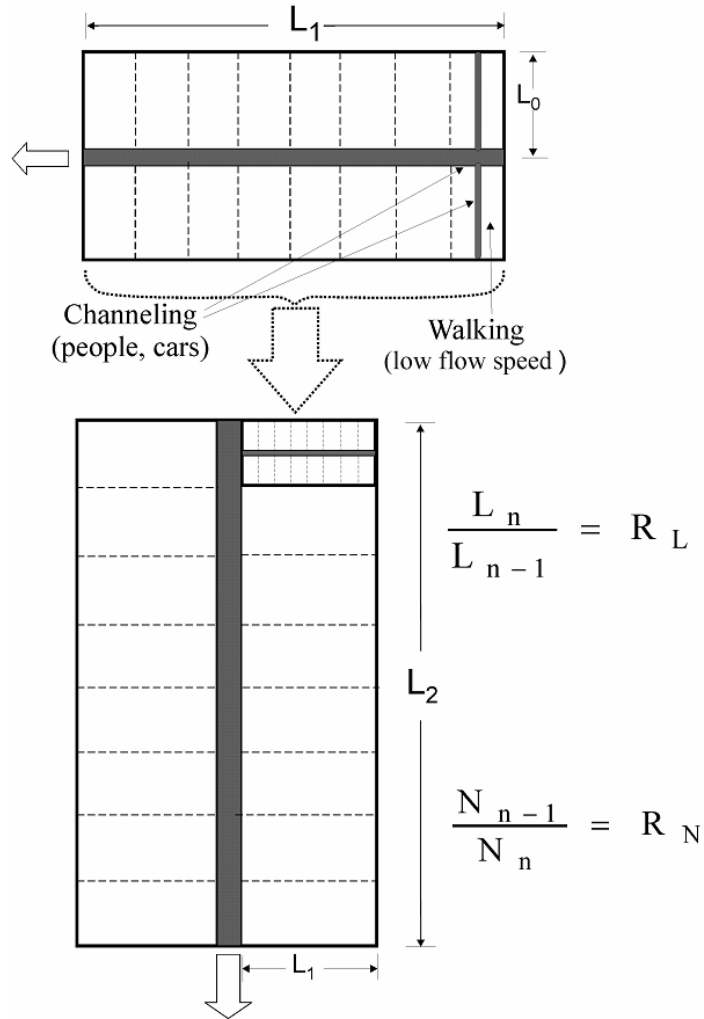
Fig. 5.4 Hierarchy of streams in a city network. People living in the area of the smallest construct (top) walk "diffusively" before reaching the first channel where the flow becomes "organized". Then, flows proceed to a larger channel (street) that is tributary of the next order channel (bottom). Known scaling laws (constant ratio between consecutive channel lengths and consecutive numbers of channels) emerge from flow access optimization.

Because these scaling laws emerge from the optimization process carried out under the eq, (11) that hold for both Hagen-Poiseuille flow and street flow (cars, people) it follows that Eqs. (12) and (13) must also hold for the city street networks. Therefore, if L_0 represents the scale of the largest stream in the city, from eq. (12) one obtains the following scaling law:

$$L_n = L_0 \big/ R_L{}^n \tag{14}$$

Analogously, from eq. (13) one obtains:

$$N_n = N_0 \big/ R_N{}^n \tag{15}$$

Taking into account eq. (14), by denoting $N(L_n) = N_n$ and $N(L_0) = N_0$ and aplying eq. (1) one has:

$$N(L_n) = N(L_0 R_L^{-n}) = R_L^{-mn} N(L_0) \tag{16}$$

or,

$$N(L_n) = (R_L^{-mn} R_N^{n}) N(L_0) / R_N^{n} \tag{17}$$

Then, by comparing with eq. (15) one obtains the fractal dimension as:

$$m = \frac{\log R_N}{\log R_L} \sim 2 \tag{18}$$

which indicates that the fractal dimension must approach 2 for a city that developed its street network under the purpose of optimizing flows of people and goods. Of course many other factors do influence city development. However, if the purpose of making city flows easier and easier is the leading one, then we do expect that the fractal dimension gets closer to 2.

Batty and Longley [14] have determined the fractal dimension of cities by using maps from different years. They found values typically between 1.4 and 1.9. London's fractal dimension in 1962 was 1.77, Berlin's in 1945 was 1.69, and Pittsburgh's in 1990 was 1.78. Dimensions closer to 2 stand for denser cities.

Shen [7], carried out a study on the fractal dimension of the major 20 US cities and found that the fractal dimension, m, varied in between 1.3 for Omaha (population – 0.86 million) and 1.7 for New York City (population – 16.4 million). In the same study it is also shown that in the period 1792–1992 the fractal dimension of Baltimore has increased from 0.7 to 1.7, which indicates that the city network has been optimized in time.

Chen and Zhou [15] found that the fractal dimension of some German cities range from 1.5 (Frankfurt) to 1.8 (Stuttgart).

A systematic study on cities fractal dimension would be needed to fully confirm that cities street networks develop as predicted by the Constructal Law. However, the few results available all point to 2 as the limit of the fractal dimension of a city that would ideally developed in time under the purpose of better and better internal flow access.

City organization has changed in time according to social organization and also to external constraints (wars, trade, etc.), and its marks have been preserved in the remains, especially in the architecture, of the ancient cities. We will discuss two different schemes of planning city space as a flow structure.

The fist case is that of organization of Roman cities (Fig. 5.5). In general, these cities were built on open spaces and spread over relatively large areas. Cities were not much constrained by city walls that came later when the Roman Empire was under attack by the barbarians. The plan of the city usually followed a design in which two principal streets (*via*) cross at the middle of the city. These broad *via* received "flow" from tributaries on both sides (Fig. 5.4). This "drainage network" with multiple mouths performed very well and, surely was efficient.

With river basins, the rule of quadrupling the number of streams from one scale to the next lower scale proved to promote the best performance (Reis, 2006a; Bejan, 2007). We can detect in the ruins of some cities (see Fig. 5.6) that Roman city
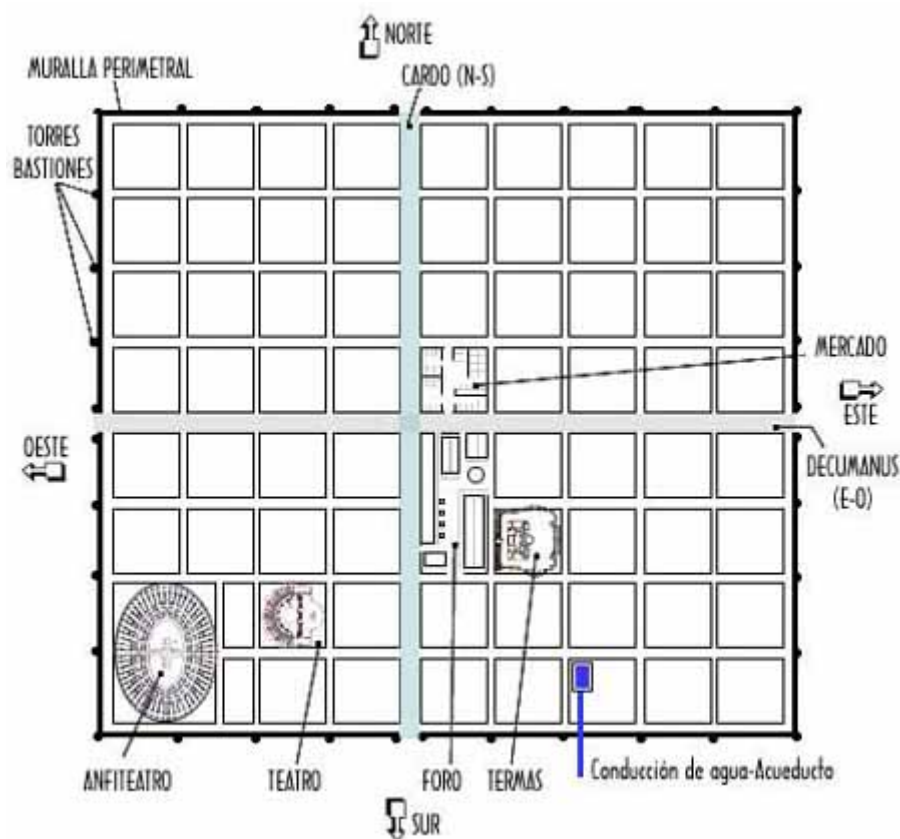
Fig. 5.5 Plan of a Roman city. The two main streets (via decumanus and cardo) cross at the center providing excellent drainage smaller street flows and flow distribution onto inside quarters. The external wall was present at the end of the Roman Empire due to the barbarian invasions.

Fig. 5.6 Ruins of the Roman city of Timgade in now Algeria (photo by A. Crosnier). Note the street network designed for near optimal flow access, very close to optimized constructal design.

planners had the intuition of the designs that promoted better efficiency with respect to city flows. Many of these designs approach the optimized constructal design of Fig. 5.4. Actually, cities in the vast territory of the Roman Empire relied on the military power of the mobile legions for defense against invasions and, usually were not much constrained by external walls. Hence, city planners had to deal mainly with the efficiency of the city network regarding flows of goods and people (merchants, horses and carriages, military personnel, etc.).

Differently from the Roman cities, the medieval ones had to face constant wars under the feudal regime and later. Defense was a major concern and therefore, almost all medieval cities developed over a small area surrounded by towering walls. Movements to the outside were usually restricted to few gates that gave controlled access to and from the outside, hence people movement was restricted to a small inside area with the market at the centre. This point to area flow and vice-versa developed special flow structures, accordingly. Fig. 5.7(a) represents the plan of a medieval city, while Fig. 5.7(b) represents the medieval city of Bologna. The flow structure developed radially, and we may speculate if such a network is a result of structure optimization in time?

Actually, the flow problem is that of optimizing point to area flow access, especially for those that lived in the periphery (circumference). Lorente et al (2002) [16] have addressed the similar problem of supplying water to users located along the edge of a circular area. The optimal flow structure, i.e. that network that supplies water without minimum resistance under the circumstances of scarcity of conduits is represented in Fig. 5.7(b). As said before, this problem is analogous to that of people that have to move between the centre and the periphery (and back) of a medieval city (usually circular in shape), facing the constraint of scarcity of free space for the movement. The flow designs of Fig. 5.7 represent almost the same flow pattern, with a so amazing similarity, that we are led to the conclusion that also medieval cities have optimized their internal street network in time.

These two examples picked from History illustrate of how in the field of social organization, namely in city organization, the "fossil" flow structures as the ancient street networks are may be understood based on principle. These examples add to many other is various fields in which the constructal law proved to be a universal principle (see Reis [17] [18]).
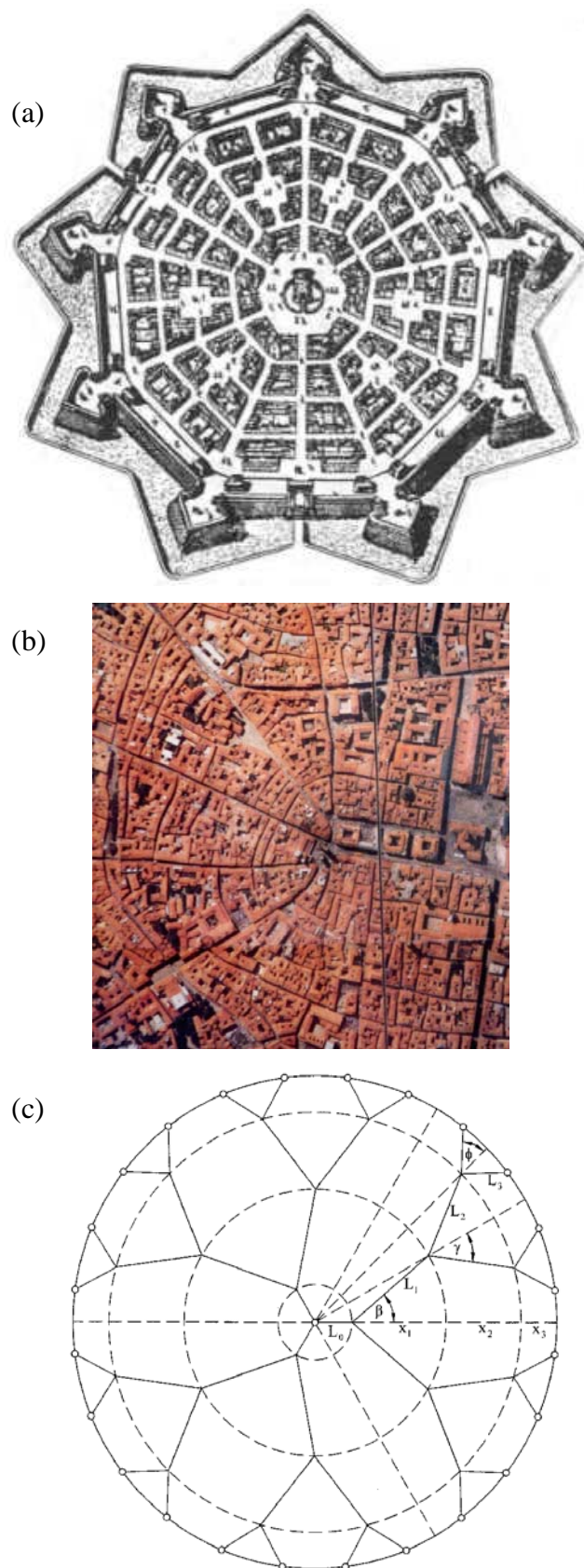
Fig. 5.7 (a) Plan of a medieval city; **(b)** Medieval Bologna (Italy).; **(c)** Constructal design for optimal flow access between the centre of the circle and points on the periphery (Lorente et al, [16]).

5.5 Conclusions

Despite few examples have been considered we believe that city networks evolve in time as the result of the continuous search for better flow configuration, therefore being a manifestation of the Constructal Law.

Analogy has been established between the scaling laws of river basins and city street networks. It was shown that city flows are governed by a law that is similar to that of channel flow. This fact provided the basis for applying the constructal relations derived for river basins to city street configuration. It was found that self-similarity appears at the various scales while the fractal dimension must be 2, ideally.

The results seem to corroborate that well developed cities tend to approach fractal dimension 2 as anticipated by the Constructal law. More, as cities develop in time and become more and more complex the fractal dimension tends to increase.

These results add to many others that confirm that wherever something flows, flow architectures emerge, which can be understood in the light of Constructal Law. Transportation networks where goods and people flow have been developed for the purpose of maximum access or best performance in economics and for facilitating all human activities. Similarly, internal flow structures where energy, matter and information flow are at the heart of engineered systems. Everything that flowed and lived to this day to "survive" is in an optimal balance with the flows that surround it and sustain it. This balancing act — the optimal distribution of imperfection — generates the very design of the process, power plant, city, geography and economics.

References

[1] L. Krier, Architecture: Choice or Fate, Andreas Papadakis, Windsor, Berkshire,England (1998).

[2] C. Alexander, S. Ishikawa, M. Silverstein, M. Jacobson, I. Fiksdahl-King, and S. Angel, A Pattern Language, Oxford University Press, New York (1977).

[3] N. A. Salingaros, "The Laws of Architecture from a Physicist's Perspective", Physics Essays **8**, (1995) pp. 638-643.

[4] M. Batty and P. A. Longley, Fractal Cities: A Geometry of Form and Function, Academic Press (1994).

[5] M. Batty and Y. Xie, Preliminary evidence for a theory of the fractal city, Environ. and Planning A, 28 (10) (1996) pp. 1745-1762

[6] N. A. Salingaros and B. J. West, A Universal Rule for the Distribution of Sizes, Environ. and Planning B **26**, (1999) pp. 909-923.

[7] G. Shen, Fractal dimension and fractal growth of urbanized areas. Int. J. Geographical Information Sc., 16 (5) (2002) pp. 419-437.

[8] R. Carvalho and A. Penn, Scaling and universality in the micro-structure of urban space, Physica A, Stat. Mech.and its Appl. 332, (2004) pp. 539-547.

[9] N. J. Moura and M. B. Ribeiro, Zipf law for Brazilian cities, Physica A, Stat. Mech.and its Appl., 367, (2006) pp. 441-448.

[10] A. Bejan, Adv. Eng. Thermod., 2nd ed., Wiley, New York, (1997) Chap. 13.

[11] A. H. Reis, Natural flow patterns and structured people dynamics – a Constructal view, in Constructal Theory of Social Dynamics, A. Bejan and G. Merkx, Eds. Springer, New York (2007).

[12] N. A. Salingaros. Principles of Urban Structure, Techne Press, Amsterdam, Holland (2005).

[13] A. Bejan, Shape and Structure, From Engineering to Nature, Cambridge University Press, Cambridge, UK (2000).

[14] A. H. Reis, "Constructal view of scaling laws of river basins", Geomorphology, 78, (2006) pp. 201-206.

[15] Y. G. Chen and Y. Zhou, Reinterpreting central place networks using ideas from fractals and self-organized criticality, Environ. and Planning B – Planning & Design, 33 (3), (2006), pp 345-364.

[16]Lorente, S., Wechsatol, W. and Bejan, A. (2002) Tree-shaped flow structures designed by minimizing path lengths, *Int. J. Heat Mass Transfer*, **45**, pp. 3299-3312.

[17] Reis, A. H., (2006b), "Constructal Theory: From Engineering to Physics, and How Flow Systems Develop Shape and Structure", *Applied Mechanics Reviews*, Vol.59, Issue 5, pp. 269-282

[18] Reis, A. H. (2008), Constructal view of the scaling laws of street networks — thedynamics behind geometry, *Physica A*, **387**, 617–622,

5. The constructal law and entropy generation minimization

Engineered systems are designed with purpose. Each system must force its flows to follow the thermo-hydrodynamic paths that serve the global objective. To select the appropriate flow paths from the infinity of possible paths is the challenge. The rate of entropy generation is a measure of how internal flows deviate from the ideal limit of flow without resistances, or without irreversibility. The constructal law calls for optimal organization that maximizes internal flow access. Optimal flow organization minimizes entropy generation and therefore maximizes the system's performance. The method of entropy generation minimization (EGM) has been recognized in engineering and is now well-established [1, 2]. Constructal theory argues that flow shapes and structures occur in nature in the same way and the principle is the constructal law.

To see the relationship between EGM and the constructal law note that the flows occurring in nature and engineered systems are dissipative. These flows generate entropy, and most may be described simply by:

$$R = V / I \qquad\qquad (1)$$

where V is the potential that drives the current I, and R is the resistance to flow. These flows generate entropy at the rate

$$\dot{S}_{gen} = VI / T \qquad\qquad (2)$$

where T is the thermodynamic temperature. Equation (12) allows us to express the resistance as

$$R = T\dot{S}_{gen} / I^2 \q\qquad\qquad (3)$$

In view of Eqs. (1) and (3), minimizing the flow resistance for a specified current I corresponds to minimizing the entropy generation rate. This shows how the constructal law and the minimization of entropy generation are connected. The constructal law goes further and focuses on the generation of the flow configuration. It brings design (drawing, architecture) in the description of flow system physics. At the same time, the connection established by Eq. (3) is a reminder that, like the constructal law, the *minimization* of entropy generation rate in flow systems is a principle distinct from the second law. This deserves emphasis: the generation of

entropy ($\dot{S}_{gen}$) is the second law, while the generation of flow configuration (e.g., the minimization of $\dot{S}_{gen}$) is the constructal law.

For illustration, consider a flow tree with N branching levels. The same current I flows in each level of branching, that is $\sum_{i=1}^{n} I_i = \sum_{k=1}^{m} I_k = I$. If at a certain level of branching, the tree has n ducts, the flow resistance at this level is

$$R = \sum_{i=1}^{n} R_i I_i / (nI) \tag{4}$$

The flow resistance at the same branching level may alternatively be expressed as a quadratic average, cf. Eq. (3),

$$R = \sum_{i=1}^{n} R_i I_i^2 / I^2 \tag{5}$$

Equations (4) and (5) lead to different values of the resistance unless $R_i I_i = V$ =const. Minimization of the tree resistance, as given by Eq. (4), at each level under the constraint of constant I, yields

$$\sum_{i=1}^{n} (R_i / (nI) - \lambda_1) dI_i = 0 \tag{6}$$

while minimization of flow resistance, as given by Eq. (5) gives:

$$\sum_{i=1}^{n} \left(2R_i / I^2 - \lambda_2 \right) dI_i = 0 \tag{7}$$

where λ_1 and λ_2 are constants. Eqs. (1)-(7) enable us to find the following relationships:

$$R_i / n = R ; \quad nI_i = I ; \quad 1/R = \sum_{i=1}^{n} 1/R_i ; \quad V = R_i I_i \tag{8}$$

In these relationships derived from the minimization of the flow tree resistance (constructal law) we can identify the well-know relationships of electric currents flowing in branched circuits. However, they hold for any tree where a current obeying Eq. (1) flows. In Eqs. (8) we find the general form of the law of equipartition of the resistances. The rate of entropy generation is constant at any branching level and is given by

$$\dot{S}_{gen} = \sum_{i=1}^{n} R_i I_i^2 / T = RI^2 / T \tag{9}$$

The minimal rate of entropy generation is given by Eq. (9) which, in view of Eq. (8), is achieved when the Eqs. (4) and (5) lead to the same resistance [3]

The great physicist Feynman noted that "....minimum principles sprang in one way or another from the least action principle of mechanics and

electrodynamics. But there is also a class that dos not. As an example, if currents are made to go through a piece of material obeying Ohm's law, the currents distribute themselves inside the piece so that the rate at which heat is generated is as little as possible. Also, we can say (if things are kept isothermal) that the rate at which heat is generated is as little as possible...." (Feynman [4]). Actually, the principle of least action accounts for point-to-point motion and cannot accommodate point-to-area and point-to-volume flows.

In summary, the constructal law provides a unifying picture for point-to-area and point-to-volume flows. It also makes clear why living organisms in their struggle for lowering the rate of internal entropy generation have constructed flow trees for optimal flow access throughout their bodies, and throughout their societies.

References

[1] A. Bejan, *Entropy Generation Through Heat and Fluid Flow*, Wiley, New York, 1982.

[2] A. Bejan, *Entropy Generation Minimization*, CRC Press, Boca Raton, 1996.

[3] A. Heitor Reis, 2006, "Constructal Theory: From Engineering to Physics, and How Flow Systems Develop Shape and Structure", *Applied Mechanics Reviews*, Vol.59, Issue 5, pp. 269-282.

[4] R. P. Feynman, R. B. Leighton and M. Sands, *"The Feynman Lectures on Physics"* 6th Ed., Vol II, Ch. 19, Wiley, 1977.

6. How the constructal law fits among other fundamental principles

System evolution in space and time is governed by fundamental principles. Classical and relativistic dynamics, electromagnetism and non-relativistic quantum mechanics spring out of the principle of least action (Feynman [1]). Symmetry is another fundamental concept evinced by Noether's theorem, which states, *"Every continuous symmetry of the dynamical equations and potential of the system implies a conservation law for the system"* (e.g. symmetry under time reversal implies conservation of energy, translational symmetry implies conservation of linear momentum, etc.) (see Callen [2]). Classical optics follows from the principle of minimum travel time taken by light between two points. The second law governs internal evolution of isolated systems by defining the sequence of equilibrium states that match successive relaxation of internal constraints.

Symmetry and the principles of least action and minimum travel time account for *motion from point to point*. The second law predicts properties of systems at equilibrium. None of these principles rationalises the occurrence of shape and non-equilibrium internal (flow) structure of systems. In fact, these geometrical features are assumed in advance as constraints to the system dynamics. In spite of being ubiquitous in nature, they are considered to be the result of chance.

Constructal theory accounts for the huge variety of natural structures and shapes and unifies them in the light of the constructal law. Chance leaves its mark in every natural system, but determinism plays here the fundamental role. The field of application of the constructal law is disjoint to those of other principles as is in the heart of non-equilibrium, flow systems, entropy generation, and evolution in time. Unlike minimum travel time and least action principles that account for motion from point to point, the reach of constructal theory is far broader. It addresses motion from volume (or area) to point and vice-versa. The principle of least action constraints motion from point to point to follow a special trajectory among an infinity of possible trajectories, while the constructal principle organizes motion from volume (or area) to point in a special flow architecture out of infinity possible architectures.

Natural systems are complex and change in many ways. In the past, scientists realized that for understanding nature they had to focus their attention on simple and homogenous systems. Motion, as the change of relative position with time, is the ubiquitous phenomenon that called for explanation, and the principle of least action is the principle that unified motions from point to point in a common picture. The constructal law is its counterpart, by allowing systems with complex internal flows to be described and understood under a unified view.

Unlike the usual direction of scientific inquiry, which divides systems into smaller and simpler sub-systems (*analysis*), constructal theory proceeds from the elemental to the complex by successively assembling blocks (*construction*), which are elemental at the stage considered but are structured and complex when viewed from the previous stage.

The parallelism between engineering and nature becomes evident (e.g., ref. [3, 4]). Engineers create systems with purpose and try to increase their performance in time. Systems have to evolve in time to approach this goal because reaching optimal performance takes time. Natural systems, animate and inanimate, also exist with purpose. The purpose of a stem is to hold and provide leaves with water and nutrients while that of river basins is to collect superficial water and deliver it into oceans. Unlike engineering, nature has been morphing its shapes and structures for billions of years. Nature uses not method, but time, evolution, tries, errors, and selecting every time the solutions that bring it closer to better flow access. Nevertheless, as parts of each of us (man + machine species), engineered systems evolve according to the same law as natural flow systems, which goes to show that to engineer is natural.

References

[1] R. P. Feynman, R. B. Leighton and M. Sands, "*The Feynman Lectures on Physics*" 6th Ed., Vol II, Ch. 19, Wiley, 1977.

[2] H. B. Callen, *Thermodynamics and an Introduction to Thermostatistics,* 2nd Ed., Wiley, New York, 1985.

[3] A. K. Pramanick and P. K. Das, "Note on constructal theory of organization in nature", *International Journal of Heat and Mass Transfer*, Vol. 48, 2005, pp. 1974-1981.

[4] G. Upham and J. Wolo, "Coordination of dynamic rehabilitation experiments of people living with Post-Polio Syndrome and call for research into PPS as a forgotten disease", *Global Forum for Health Research*, Mexico, November 2004, http://www.globalforumhealth.org/forum8/forum8-cdrom/Posters/Upham%20G%20F8-203.doc

8. Conclusion

There is no limit to this subject. It is just a different point of view of things, which constructal theory proposes. It is a point of view of the engineer about the forms of nature. Constructal theory proposes to see the trees, the human bodies, like machines that are subjected to constraints, which are constructed with a goal, an objective, which is to obtain maximum efficiency.

This constructal theory is about the method of constructing such machines, which attain optimally their objective. It proposes a different look at corals, birds, atmospheric flow and, of course, at the machines built by engineers.

In this paper we gave an overview of the applications of the constructal theory, which extends from engineering to natural systems, alive and inanimate and to human activities like organization of cities, transportation and economics. Wherever something flows, a flow architecture emerges, which can be understood in the light of constructal theory. The many examples presented here illustrate how the symbiosis between flow dynamics and geometry is the heart of constructal theory. This theory has proved to be useful in describing complex flow systems and the field of its potential applications is open to researchers from engineering and natural and social sciences. In my view, constructal theory is essential to those who strive to describe natural systems in a quantitative fashion.

Constructal theory also provides a new way of thinking with epistemological and philosophical implications (Rosa [1], Patrício [2], T. M. Bejan [3]). From the epistemological point of view, its method proceeds from the simple to the complex, against the usual paradigm of science that calls for the deconstruction of the complex to reach the elemental. The philosophical consequences are also obvious and important: constructal theory gives chance a secondary role in the evolution of natural systems. Constructal theory assigns the major role to determinism, and contributes significantly to the debate on the origin of living systems.

[1] R. Rosa, Preface in *Bejan's Constructal Theory of Shape and Structure*, pp. 15-47, R. Rosa, A. H. Reis and A. F. Miguel, Edts., Évora Geophysics Centre, Évora, 2004.
[2] M. F. Patrício, Foreword in *Bejan's Constructal Theory of Shape and Structure*, pp. 1-3, R. Rosa, A. H. Reis and A. F. Miguel, Edts., Évora Geophysics Centre, Évora, 2004.
[3] T. M. Bejan, "Natural Law and Natural Design", *Dogma*, http://dogma.free.fr, Feb. 2005.